

## Student Research Project

# Mmwave Transceiver System Performance Analysis using Post-Processing ~~Analysis~~

Digital Post Processing Techniques

Yang Liu

Supervisor: Prof. Dr.-Ing. Ingmar Kallfass  
M. Sc. Seyyid Muhammed Dilek

Period: Still didn't find a way to delete it – 31.07.2018

Stuttgart, 31.07.2018



## **Declaration**

I hereby declare that this thesis is my own work and effort and follows the regulations related to good scientific practice of the University of Stuttgart in its latest form. All sources cited or quoted are indicated and acknowledged by means of a comprehensive list of references.

Stuttgart, 31.07.2018

Yang Liu



## Executive Abstract

Performance enhancement of a millimeter-wave transceiver system is a challenging problem in modern radio ranging, detection, and communication applications which in fact make this problem motivational to work on. Digital post-processing techniques which use adaptive equalization filters are an important way to improve performance for broadband millimeter-wave wireless transceiver system. Digital post-processing methods can dramatically improve the performance of the received digital baseband signal and, furthermore, it can mitigate the analog front-ends and channel impairments influence. Analog front-ends and channel non-idealities for transceiver systems concern the performance degradation of the signal quality. There are various ways for the mitigation techniques which is explained in this research thesis.

### driving researchers to study towards

The growth of Internet traffic and network connections are driving researchers towards millimeter-wave between 30 GHz and 300 GHz. Among this RF range, E-band (71-76 GHz and 81-86 GHz) receives particular attention and provides new potentials and challenges for providing affordable and reliable point-point communications with data rates up to  $10 \text{ Gbits}^{-1}$ . However, higher frequencies of mmW raise strong requirements on low transmission distortion and high impairment mitigation ability at pose-end. This thesis first reviews the available bandwidth and regulation in the E-band. Subsequently, different analog front-ends and channel impairments are studied along the causes and classifications.

Based on properties and classifications, applicable post-processing methods are realized and simulated to evaluate its performance. For deterministic impairments, linear adaptive filters, including LMS, RMS, CMA etc. performance a satisfied improvement after convergence. For stochastic impairments, basic machine learning method such as KNN and SVM are tested as a primary trial. Several distortions are equalized effectively and EVM is reduced from 34 % to 4 %. In the consideration of practice, optimized parameters and recommendations are given. Different adaptive algorithms are also compared in terms of computational load. Finally, it is argued that the related post-processing methods can be used to enhance the performance of broad-band mmW transceiver system, although the algorithms in the application should be optimized to reduce the computational complexity.



## **Zusammenfassung**

Today Finish the Deutsch version of Abstract



# Contents

<b>List of Abbreviations</b>	<b>iii</b>
<b>List of Figures</b>	<b>vi</b>
<b>List of Tables</b>	<b>vii</b>
<b>1 Introduction</b>	<b>1</b>
<b>2 Fundamentals</b>	<b>5</b>
2.1 Receiver Architecture . . . . .	6
2.2 Figures of Merit . . . . .	8
2.2.1 Signal Noise Ratio . . . . .	8
2.2.2 Bit Error Ratio . . . . .	8
2.2.3 Symbol Error Rate . . . . .	9
2.2.4 Adjacent Channel Power Ratio . . . . .	10
2.2.5 Waveform Quality Factor ( $\rho$ ) . . . . .	11
2.2.6 Modulation Error Rate . . . . .	12
2.2.7 Eye Diagram . . . . .	12
2.2.8 Noise Power Ratio . . . . .	13
2.2.9 Error Vector Magnitude . . . . .	14
2.3 Classification of Impairments . . . . .	17
2.3.1 Deterministic and Stochastic System Definition . . . . .	17
2.3.2 Linear and Nonlinear System . . . . .	19
2.3.3 Time-Invariant and Time-Varying System . . . . .	19
2.4 Deterministic Impairments . . . . .	20
2.4.1 IQ Imbalance . . . . .	20
2.4.2 Carrier Feedthrough/Leakage, IQ Offset, DC Offset . . . . .	21
2.4.3 Amplitude/Phase Response depending on frequency . . . . .	21
2.4.4 Multipath Propagation . . . . .	22
2.4.5 Intersymbol Interference (ISI) . . . . .	23
2.4.6 Inter-Modulation (IM) distortion . . . . .	24
2.5 Stochastic Impairments . . . . .	24
2.5.1 Phase Noise . . . . .	24
2.5.2 Additive White Gaussian Noise . . . . .	25

---

<b>3 Theory of Post Processing Methods</b>	<b>27</b>
3.1 Adaptive Filter Theory . . . . .	27
3.1.1 Linear Adaptive Filters . . . . .	28
3.1.2 Supervised Adaptive Filter Algorithm . . . . .	29
3.1.3 Blind Adaptive Filtering . . . . .	32
3.2 Machine Learning Method . . . . .	34
3.2.1 $k$ -nearest neighbors (KNN) Method . . . . .	34
3.2.2 Support Vector Machine (SVM) Method . . . . .	35
<b>4 Filters Design and Simulation Results</b>	<b>39</b>
4.1 Received Signal Generator . . . . .	39
4.2 Convergence Analysis . . . . .	40
4.2.1 Supervised Adaptive Compensator: Least Mean Square (LMS) and Recursive Least Squares (RMS) . . . . .	40
4.2.2 Blind Adaptive Compensator: Constant Modulus Algorithm (CMA) and modified CMA . . . . .	42
4.2.3 Blind Adaptive Compensator: Circularity-Based Approach . . . . .	45
4.3 Impact of the Hyperparameters . . . . .	45
4.4 Computational Load and Impact of time-varying channels . . . . .	48
4.5 KNN and SVM Detectors . . . . .	50
<b>5 Conclusion and Perspectives</b>	<b>53</b>
<b>Bibliography</b>	<b>53</b>
<b>Appendices</b>	<b>57</b>
<b>Appendix A Acknowledgments</b>	<b>59</b>
<b>Appendix B Script Flow Chat</b>	<b>61</b>
<b>Appendix C Simulation Results</b>	<b>63</b>

## List of Abbreviations

ACPR	Adjacent Channel Power Ratio
ADC	Analog-to-Digital Converter
ADS	Advanced Design System
AWGN	Additive White Gaussian Noise
BER	Bit Error Ratio
CFD	Cumulative Distribution Function
CMA	Constant Modulus Algorithm
EVM	Error Vector Magnitude
FCC	Federal Communications Commission
IF	Intermediate Frequency
ILH	Institute of Robust Power Semiconductor Systems ( <i>Institut für Robuste Leistungshalbleitersysteme</i> )
IM	Inter-Modulation
IQ	in-phase and quadrature
ISA	International Standard Atmosphere
ISI	Intersymbol Interference
KNN	$k$ -nearest neighbors
LMS	Least Mean Square
LO	Local Oscillator
LTI	Linear Time-Invariant
LTV	Linear Time-Varying
MER	Modulation Error Rate
ML	Machine Learning
mmW	millimeter-wave
MSE	mean squared error
NPR	Noise Power Ratio
PA	Power Amplifier
PDF	Probability Density Function
QAM	Quadrature Amplitude Modulation
QPSK	Quadrature Phase-Shift Keying
RF	Radio Frequency
RMS	Recursive Least Squares
SER	Symbol Error Rate
SNR	Signal Noise Ratio

SVM      Support Vector Machine

# List of Figures

1.1	Global Internet Traffic Statistic Data and Prediction by Year . . . . .	1
1.2	Atmospheric attenuation for electromagnetic wave propagation at International Standard Atmosphere (ISA) conditions and at a typical water vapor density of $7.5 \text{ g m}^{-3}$ [own depiction, curves are calculated from [1]] . . . . .	3
2.1	Simplified architecture of the super-heterodyne receiver with dual down-conversion, BP: Bandpass, LNA: Low Noise Amplifier, VCO: Voltage Controlled Oscillator, ADC: Analogue Digital Converter, DSP: Digital Signal Processor . . . . .	6
2.2	Spectrum Shifting in Superheterodyne with Nyquist Intermediate Frequency (IF) Sampling, $F_{\text{LO}} = F_c + \frac{3F_s}{4}$ . . . . .	7
2.3	Simplified architecture of zero-IF approach . . . . .	7
2.4	Spectrum Shifting in Direct-Conversion/Zero IF, $F_{\text{LO}} = F_c$ . . . . .	8
2.5	Approximation of bit error probabilities of M-QAM over AWGN channel (for no channel coding, i.e., $R_c = 1$ ) . . . . .	9
2.6	16-Quadrature Amplitude Modulation (QAM) Modulation in Gray code. Black dots are the ideal constellation, green dots as correctly decoded symbols and red dots as wrongly decoded symbols . . . . .	10
2.7	The Definition of ACPR . . . . .	11
2.8	Schematic diagram of Modulation Error Rate (MER) . . . . .	13
2.9	Interpretation of eye diagram, <i>a</i> : Time interval for sampling, <i>b</i> : Distortion of zero crossings, <i>c</i> : Noise margin at best sampling time, <i>d</i> : Distortion at sampling instant .	13
2.10	Definition of NPR . . . . .	14
2.11	Vectorial Representation of Error Vector Magnitude. . . . .	15
2.12	Classification of Analog Front-End and Channel Error Sources . . . . .	17
2.13	Block Diagram of the Stochastic System . . . . .	18
2.14	Additive White Gaussian Noise (AWGN) Channel . . . . .	26
3.1	FIR Transversal Structure . . . . .	28
3.2	Basic SVM Concept with support vectors in circles . . . . .	36
3.3	Linear inseparable points in low dimension (2-D) become separable in higher dimensions (3-D) . . . . .	37
4.1	Supervised Adaptive Compensator . . . . .	40
4.2	A frame structure that contains reference training signal and transmitted data . . . . .	40
4.3	Equalizer with LMS Adaptive Filter for 4-QAM . . . . .	41

4.4	<i>Eb/N<sub>0</sub></i> w/o RMS Adaptive Filter for 4-QAM . . . . .	42
4.5	RMS Expression in different IQ Imbalance, the top layer is EVM before compensation and lower layer is EVM after compensation . . . . .	43
4.6	Equalizer with CMA Adaptive Filter for 4-QAM . . . . .	44
4.7	Equalizer with Modified CMA Adaptive Filter for 4-QAM . . . . .	46
4.8	Equalizer with Circularity-Based Approach Filter for 4-QAM . . . . .	47
4.9	MSE of CMA filter in different filter length $N$ . . . . .	48
4.10	Convergence Results for Different Step Size . . . . .	49
4.11	Symbol Error Rate (SER) with and w/o KNN Detector . . . . .	51
4.12	RX Constellation Points with Phase Noise Impairment . . . . .	51
4.13	Detection of SVM against Phase Noise Impairment . . . . .	52
.1	Script Flow Chat . . . . .	61
.1	Signal with Channel Distortion . . . . .	63
.2	Signal with IQ Imbalance . . . . .	64
.3	Signal with Phase Noise . . . . .	64
.4	Signal with AWGN . . . . .	65
.5	Signal Compensated by LMS Filter . . . . .	65
.6	Signal Compensated by Circularity Approach . . . . .	66
.7	SVM Recognize . . . . .	66

## List of Tables

4.1	Simulation Condition . . . . .	39
4.2	Time Cost for Different Adaptive Filters (with optimal hyperparameters), 4-QAM . .	50



# 1. Introduction

With the explosion of demand for smartphones, mobile technology affects everyday life more than any moment in the history. People are extremely delighted by the new interactive way with another part of the world and seeking more robust but smaller and lighter devices. As the foundation of mobile life, telecommunication technology plays a key role in the new century. Mobile data traffic is growing at an extraordinary rate. According to Cisco[2], with growth of 63 % annually, global mobile data traffic reached 7.2 EB (1 EB= $10^9$  GB) per month at the end of 2016. Figure 1.1 shows this explosive growth and prediction till 2021 [2]. Almost half a billion (429 million) mobile devices and connections were added in 2016. To meet this increase in the bandwidth demand and solve the saturation problem in networks, carriers are pushed to millimeter-wave (mmW) frequency range.

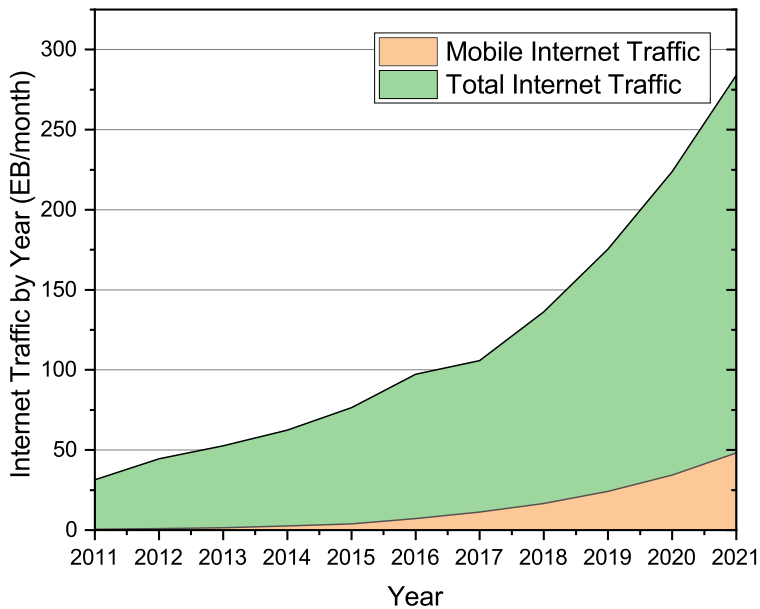


**Figure 1.1.:** Global Internet Traffic Statistic Data and Prediction by Year

The modern communication involves on electrical, electromagnetic and optical theories. The first revolution in wireless communication happened in the early 1900s. Guglielmo Marconi made an effective contribution to radio communications and won the Nobel Prize in Physics in 1909 [3]. The industry has developed rapidly from wire transmissions to radio broadcast, mobile network and satellite communications. Life and production are highly dependent on telecommunication technology, especially on cellular networks, Bluetooth and Wireless Local Area Networks (WLAN).

The next generation telecommunication standard 5G is expected to provide peak data rate as high as  $20 \text{ Gbits}^{-1}$  [4]. In order to achieve this high transmission speed, there are basically two ways: One is to increase the bandwidth; the other is to improve spectrum utilization.

After Federal Communications Commission (FCC) of the United States announced the availability of spectrum in 71-76 GHz, 81-86 GHz (both referred as E-band) in 2003, E-band is permitted worldwide for high capacity wireless point-to-point communications [5]. Many parts of the world followed the US and European and opened up the E-band frequencies for high capacity peer-to-peer communication. The overall 10GHz wide-band spectrum is the widest bandwidth allocated up to now and enabling GB-speed transmission through millimeter-wave [6]. The allocation of E-band has many advantages. They are summarized in the following:

Firstly, the combined 10GHz is over 50-times larger than the entire spectrum allocated for all generations of cellular services. The ability of such a large spectrum enables a whole new generation of wireless transmission.

Secondly, the E-band allocation is not further partitioned than two paired 5GHz. While each common carrier microwave band is divided into channel no more than 50MHz, E-band has 100-times the size of even the largest microwave band [7]. With efficient modulations, full data rates of 10GHz can be realized. Since there is no need to compress the data into IF, systems can be implemented by relatively simple architectures, which can reduce system cost and complexity.

Thirdly, wireless propagation at E-band frequencies is well studied. The atmospheric attenuation of radio waves varies significantly with frequency as Figure 1.2 shows. The vertical gray band is the E-band frequency. At the microwave frequency bands up to 30GHz, the attenuation is lower than  $0.1 \text{ dB km}^{-1}$  due to the atmosphere at sea level. A small peak at 23GHz is followed by a large peak at 60GHz. This two peaks significantly limits radio transmission distance and signal stability. A clear atmospheric window can be seen in the E-band spectrum. For this reason, E-band wireless systems can transmit high speed data over long significant distance.

Here the gap between two graph is less than others  
As for improving spectrum utilization, higher modulation is used at the same time. However, high-order modulation is much more sensitive than low-order modulation. Hence the compensation of different modulations and precise recognition play a critical role.

The aim of this thesis is that, after studying different front-end impairments in Radio Frequency (RF) and post-methods, realize the post-methods in MATLAB and compensate the front-end impairments. Results of compensation is also evaluated in terms of computational complexity.

Chapter 2 of this thesis explains the structure of receiver architecture, classifications and characters of analog front-end impairment. The focus of this chapter is causes and mathematical expression

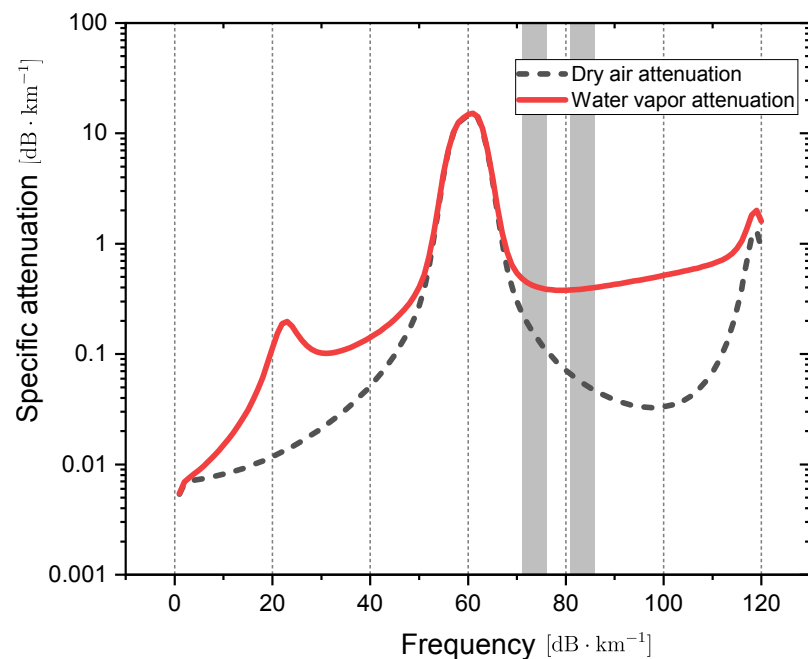


**Figure 1.2.:** Atmospheric attenuation for electromagnetic wave propagation at ISA conditions and at a typical water vapor density of  $7.5 \text{ g m}^{-3}$  [own depiction, curves are calculated from [1]]

Try to fit this photo and text together, only one graph in one page doesn't look nice

of various impairments, in order to choose the corresponding equalization method in Chapter 3. Mathematical theories and algorithms are proposed in Chapter 3. For deterministic distortion we choose adaptive filters and for stochastic impairments we apply some basic machine learning ideas. The Performance evaluation of the proposed algorithms is carried out in Chapter 4. We evaluate the equalizer performance, according the constellation, Error Vector Magnitude (EVM) and Bit Error Ratio (BER). We also propose the computational complexity and give advices for parameter choose for adaptive algorithms. Finally, in Chapter 5, conclusions are drawn and recommendations are given.

## 2. Fundamentals

The mmW spectrum offers a wide bandwidth and can enable high-data-rate wireless communications.

Connect this two paragh, make one

One of the challenges in the circuit implementation of mmW high speed transmission is the linearity/efficiency trade-off. Wireless transceiver architecture such as heterodyne receivers when applied to modern wireless systems impose heavy complexity and lack flexibility. This causes performance limitations in terms of cost, gain and noise power tradeoff. To solve this disadvantage, recent wireless systems switch from traditional heterodyne receivers to low intermediate frequency (IF) and homodyne ( also called as direct conversion or zero-IF ) receivers.

In order to measure the quality of the system, transmitters, signal paths, receivers should be quantitatively measured. So many figures of merits are discussed to indicate the quality of the transmission system. Signal Noise Ratio (SNR) and Bit Error Ratio (BER) shows the signal quality of the received signal. Adjacent Channel Power Ratio (ACPR), Error Vector Magnitude (EVM), Modulation Error Rate (MER) are used to indicate the quality of the whole transmission system in various aspects of comparing received signal and target signal in constellation plane. Sometimes two-tone IM distortion may not be indicative for multitone signals. By creating a notched signal, NPR provides an accurate prediction for multitone IM distortion. Eye diagram introduces a straightforward way to observe the information of receiving signals. It is an effective tool to provide a visual examination of the severity of the *Intersymbol Interference* (ISI), sensitivity to timing errors, and the noise margin[8].

In last part of this chapter, different impairments are briefly introduced. The attractiveness of the homodyne architecture comes with various implementation issues that mainly arise from the impairments in analog hardware in the receiver front ends. In this report, several impairments associated with those homodyne receivers as well as impairments for general receiver architectures. According to different criterion, the impairments are classified to linear and nonlinear, deterministic or stochastic, time-invariant or time-varying errors. This classification will be helpful for the further impairments handling.

## 2.1. Receiver Architecture

Modern receivers serve multiple users that operate in narrow bandwidth and require the ability to select the appropriate channel with effective interference suppression from other channels. Among various receiver architectures, two widely-used and well-known receiver architectures, i.e., heterodyne and direct-conversion receivers.

### Superheterodyne Receivers

The superheterodyne architecture was developed in 1918 by Edwin Armstrong with respect to the technical issues of implementation [9].

The basic block schematic of superheterodyne architecture depicted in Figure 2.1.

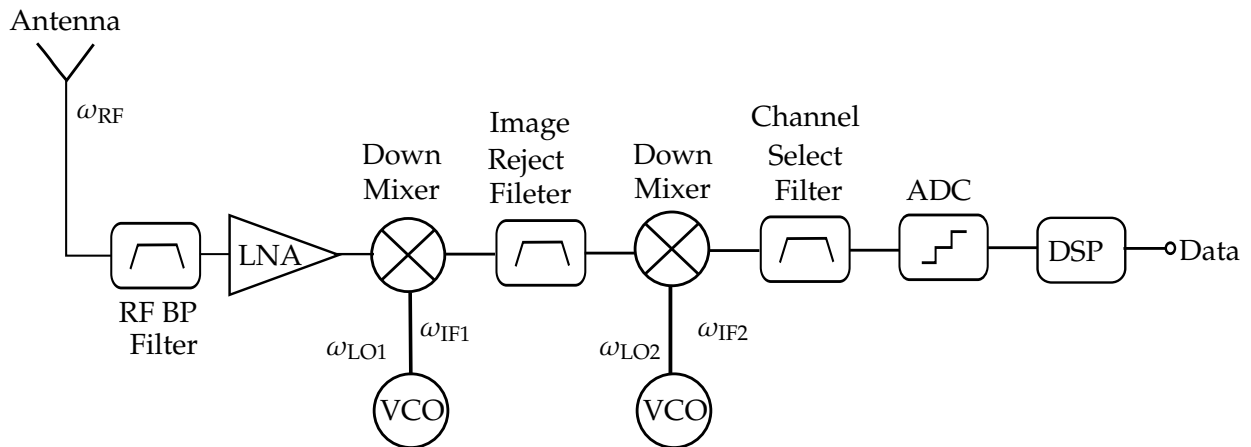


**Figure 2.1.:** Simplified architecture of the super-heterodyne receiver with dual down-conversion, BP: Bandpass, LNA: Low Noise Amplifier, VCO: Voltage Controlled Oscillator, ADC: Analogue Digital Converter, DSP: Digital Signal Processor

The resulting signal frequency is shifted down to an IF as shown in Figure 2.2. To realize this, receivers typically convert the received RF signal into IF signal by mixing RF with a Local Oscillator (LO) signal. This mixing process generates frequency components at  $f_{IF}$  and  $2f_{RF} - f_{IF}$ . The major design concern is choosing the right IF such that it is high enough to successfully reject the image band and low enough such that channel selection filters can be designed feasibly. Although heterodyne and superheterodyne architectures are long-tested and general used in industries, they show still insufficient and limitations in many aspects. The major issue arising in this type of down conversion is the so called image band problem, that is caused by the interference of the required signal with its mirror signal. To overcome this problem, image-rejection filters are applied as in Figure 2.3 before mixing the incoming signals with the local oscillator signal (LO). Secondly, this kind of architecture increases system complexity. It demands addition LO and RF mixers to convert signals from RF to IF before conversion to baseband. In terms of accessible bandwidth, the requirement of power and physical size is also large.

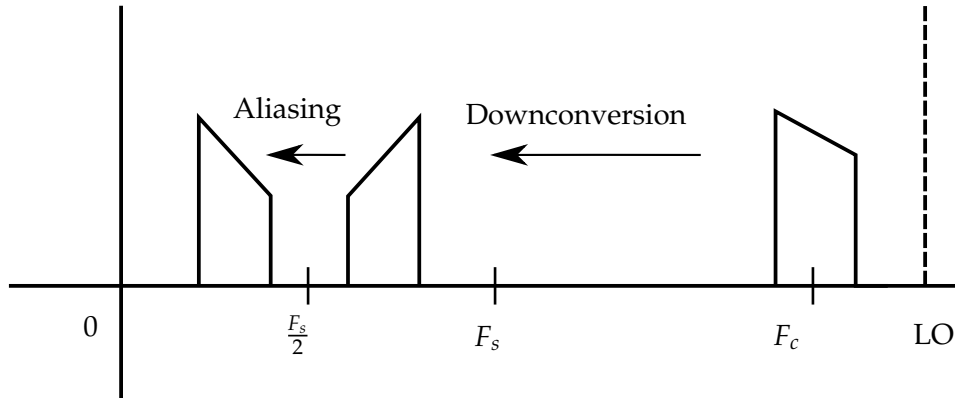


**Figure 2.2.:** Spectrum Shifting in Superheterodyne with Nyquist IF Sampling,  $F_{\text{LO}} = F_c + \frac{3F_s}{4}$

### Direct Conversion/Zero IF Receivers

Direct conversion receivers are also known as homodyne or zero-IF receivers since the resulting IF frequency is zero. Hence, the useful signal is its own image. In Figure 2.3 the typical block schematic of a direct conversion receiver is depicted.

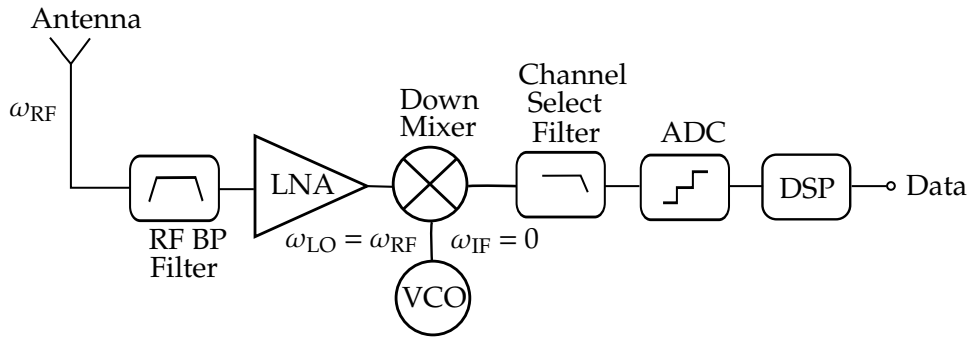


**Figure 2.3.:** Simplified architecture of zero-IF approach

As Figure 2.4 shows, the LO frequency is chosen the same as carrier frequency. Through down mixer, the RF signal is direct-down converted to baseband and ensure  $f_{\text{IF}} = 0$ .

As *Abidi* summarized in 1995 [10], the major problems of direct conversion architecture at that time are LO leakage, in-phase and quadrature (IQ) imbalance in down conversion mixer, frequency-error between LO of the transmitter and receiver. Recently with the progress of digital adjustment technology and development of integrating circuit, direct conversion architecture is already practical and reliable methods in various system.

Direct conversion architecture has many advantages over heterodyne receivers. It does not suffer from image band problem and does not require IF filters thereby hugely reducing the system complexity. Hence the power and space demands are decreases consequently. Since the requirement of filters and Analog-to-Digital Converter (ADC) in baseband is significantly reduced, low power adaptive filters and other devices can be used [10].

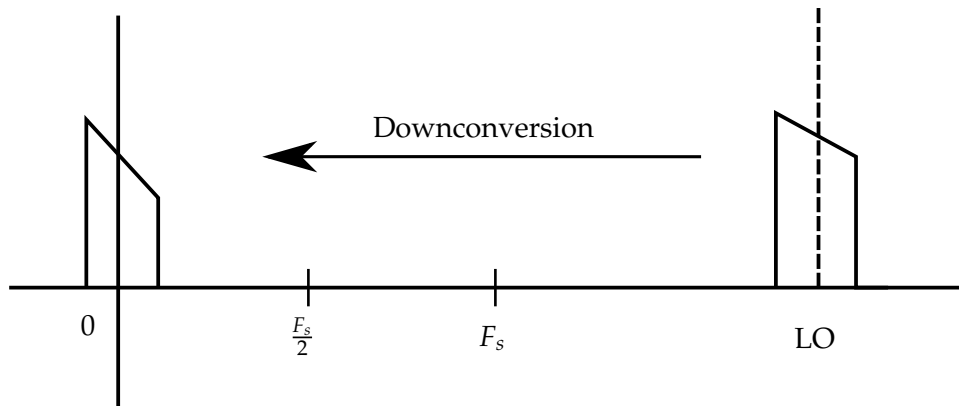


**Figure 2.4.:** Spectrum Shifting in Direct-Conversion/Zero IF,  $F_{\text{LO}} = F_c$

## 2.2. Figures of Merit

Wireless communication system performance can be characterized by different figures of merit. Besides the often used SNR, other system metrics are also used to quantify system performance and can be more effective and also related to SNR.

### 2.2.1. Signal Noise Ratio

The SNR is a basic indication of impairments used in engineering that compares the level of a desired signal to the stage of background noise. It is defined often in decibels by a ratio value between the power of the signal and of noise as

$$\text{SNR} = \frac{P_{\text{signal}}}{P_{\text{noise}}}. \quad (2.1)$$

$P_{\text{signal}}$  and  $P_{\text{noise}}$  are the power of signals and of noise. A positive SNR higher indicates more signal than noise.

### 2.2.2. Bit Error Ratio

BER is the main performance parameter of a wireless channel and is defined as the number of error bits found in a given bit sequence at the receiver end.

$$\text{BER} = \frac{N_{\text{error}}}{N_{\text{total}}} \quad (2.2)$$

BER depends on the value of SNR. It decreases with the increase in SNR[11] as Figure 2.5 shows.

Communication service quality can be described by the average BER. Typically, a BER of  $10^{-2}$  or better is required for voice telephony, and  $10^{-5}$  or better is required according to [12]. Different modulation schemes require more or less power to achieve the same bit error rate. As the re-

quirement of transmission speed, higher modulation increases bit error rate and the higher SNR is demanded satisfied the requirement of BER.

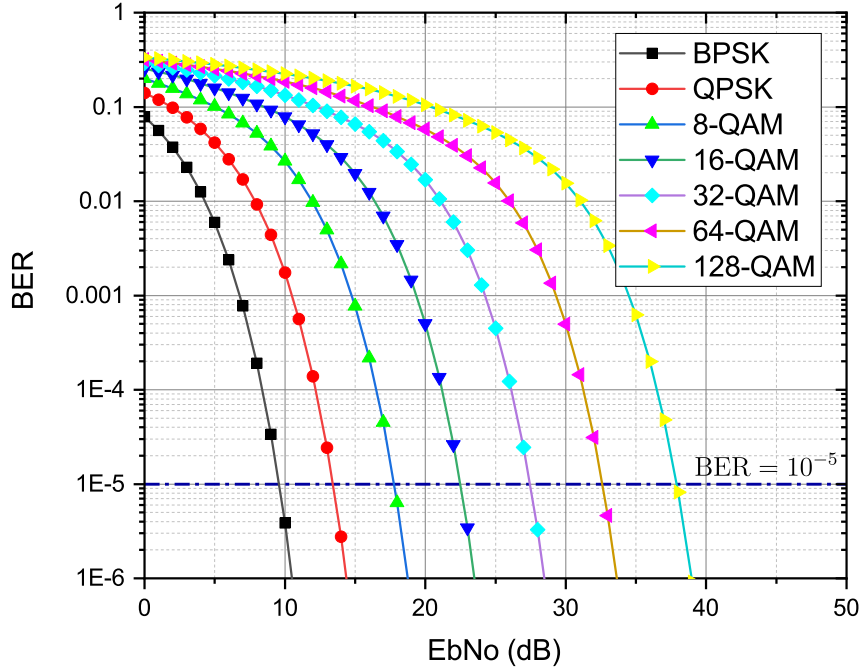


**Figure 2.5.:** Approximation of bit error probabilities of M-QAM over AWGN channel (for no channel coding, i.e.,  $R_c = 1$ )

### 2.2.3. Symbol Error Rate

When transmitting a data stream, symbols are often used instead of individual bits. In terms of modulation scheme, each symbol carries several bits. The transformation from bits to corresponding symbols is called demodulation. SER is the ratio of the number of wrong demodulated received symbols to the total number of transferred symbols. There is no strict identification between SER and BER. However, their approximations can be accurate enough in terms of coding as

$$BER \approx \frac{SER}{\log_2 M}. \quad (2.3)$$

Gary coding is widely used in the correspondence of symbol and bit since neighboring symbol differs only 1 bit from each other. Figure 2.6 shows constellation diagram in 16-QAM. Black dots are the ideal constellation. Assuming that a lot of symbols (1, 1, 1, 1) are sent, they can be received out of the right area because of various distortion. Green dots are demodulated correctly and red dots will become wrongly demodulated symbols, which is namely symbol errors.

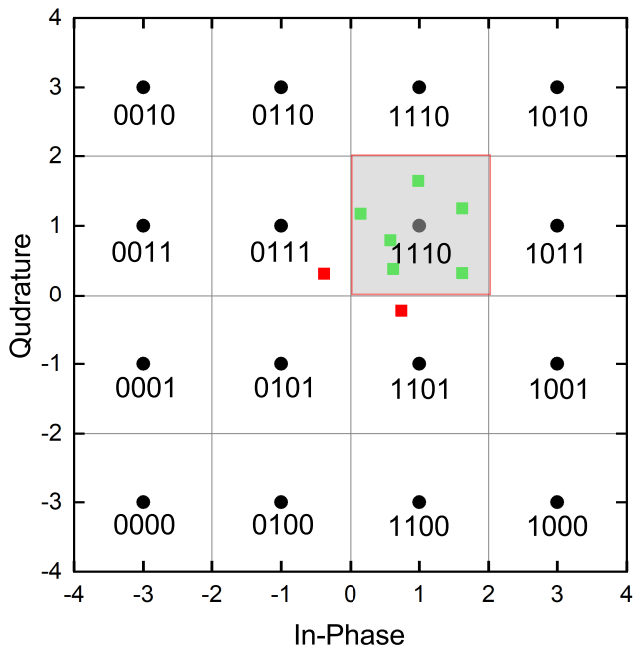


**Figure 2.6.:** 16-QAM Modulation in Gray code. Black dots are the ideal constellation, green dots as correctly decoded symbols and red dots as wrongly decoded symbols

#### 2.2.4. Adjacent Channel Power Ratio

In the communication system, the signal should be transmitted in a limit frequency (channel bandwidth). However, because of the IM distortion, a series of harmonic signals in similar frequencies cause a lot of IM signals inside and out (adjacent-channel) of the channel. Resulting from nonlinear amplification in wireless communication systems there is spectral broadening called Adjacent-Channel Interference (ACI). Both an in-band distortion and an out-of-band distortion exist.  $P_{1dB}$  which is measured by using a single-tone signal, and third-order interception point, which is acquired by using a two-tone signal, are not adequate for metrics of Power Amplifier (PA) nonlinearities. Because modern RF waveforms are digital modulated signals that use complex modulations and have different signal statistics from single-tone or two-tone signals. Since other frequencies can also be used by other communication systems, ACI causes noise in other neighbor channels. So it's necessary to establish a lower limit on the ratio of the power in the main channel to the amount of power induced in the adjacent channel.

The power ratio of main channel to the adjacent-channel is called Adjacent-Channel Power Ratio (ACLR), which is defined as

$$ACPR = \frac{\int_{f_1}^{f_2} S_{yy}(f) df}{\int_{f_3}^{f_4} S_{yy}(f) df}. \quad (2.4)$$

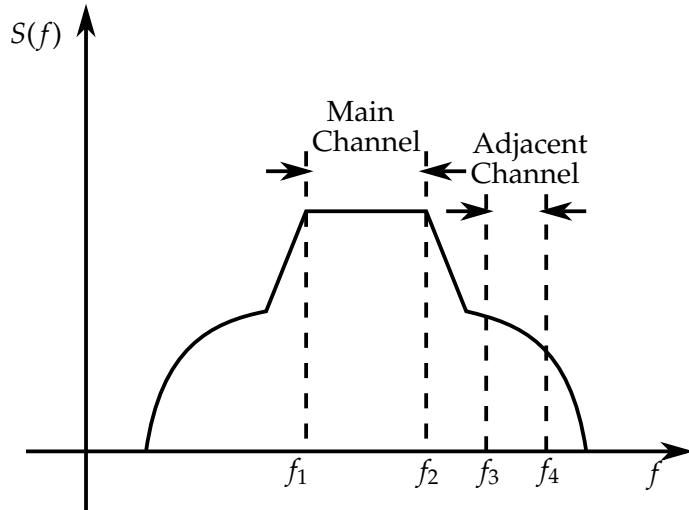


**Figure 2.7.: The Definition of ACPR**

The frequencies  $f_1$  and  $f_2$  are the frequency limits of the main channel, while  $f_3$  and  $f_4$  are the limits of the upper adjacent channel.

ACPR describes linearity of the communication system with the influence of third order intermodulation distortion. The poor CPR means that some energy that is supposed to be in main channels leaked to adjacent channels. It results in reducing the efficiency of signal transmissions.

### 2.2.5. Waveform Quality Factor ( $\rho$ )

In the CDMA system, the waveform quality factor  $\rho$  is used to represent the modulation accuracy instead of EVM[13]. The waveform quality factor is a measure of the correlation between a scaled version of the input and the total in-channel output waveforms. The waveform quality factor  $\rho$  [14] is defined as a correlation coefficient between the actual waveform  $Z(t)$  and the ideal waveform  $R(t)$ , and it is expressed as

$$\rho = \left( \frac{\sum_{k=1}^M R_k Z_k^*}{\sum_{k=1}^M R_k \sum_{k=1}^M Z_k} \right)^2, \quad (2.5)$$

where  $R_k = R_k(t_k)$  is the  $k$ th sample of the ideal signal in the measurement interval;  $Z_k = Z_k(t_k)$  is the  $k$ th sample of the actual signal in the measurement interval; and  $M$  is the measurement interval in half-chip intervals. There is an approximate relationship between  $\rho$  and the EVM when the cross-correlation between the ideal signal and the error signal is negligible,

$$\begin{aligned} \rho &= \frac{1}{1 - EVM^2} \\ &= \frac{SNR}{SNR + 1} \end{aligned} \quad (2.6)$$

### 2.2.6. Modulation Error Rate

MER is an important qualitative parameter for transmission quality of RF modulation. Similar to EVM, MER expresses the difference between the ideal complex voltage value and the value of the actual received symbol.

QAM can be expressed in an analog way by constellation diagram and also in a digital way by two digital bit streams. The two carrier waves are with a phase difference of  $90^\circ$  and are called quadrature components of I component and Q component. All constellation points, which are I and Q components, will precisely locate an ideal location, if the transmitter, signal path, and receiver are all ideal. However various imperfections in the implementation such as noise, phase noise, carrier suppression, etc. cause the shift between the actual and ideal constellation points.

As shown in Figure 2.11, modulation error is expressed as the error vector in the IQ plane. MER formula can be presented as

$$\begin{aligned} MER(\text{dB}) &= 10 \log \frac{P_{\text{average signal}}}{P_{\text{average error}}} \\ &= 10 \log \left( \frac{\sum_{j=1}^N (\tilde{I}_j^2 + \tilde{Q}_j^2)}{\sum_{j=1}^N [(I_j - \tilde{I}_j)^2 + (Q_j - \tilde{Q}_j)^2]} \right) \end{aligned} \quad (2.7)$$

where  $N$  is the number of measurements,  $\tilde{I}_j$  and  $\tilde{Q}_j$  are the ideal components of  $j$ -th symbol;  $I_j$  and  $Q_j$  are the measured components of  $j$ -th symbol. This definition assumes that a long enough sample is taken so that all the constellation symbols are equally likely to occur. So the higher MER value means the better RF modulation performs. Figure 2.8 expresses a large "cloud" of symbol points equates to low MER value, which is not good. The right part is what is wanted, a small "cloud" and high MER value.

### 2.2.7. Eye Diagram

Eye diagram generation is a straightforward and visual figure of merit. It provides an effective tool for the severity of ISI, sensitivity to timing errors and noise margin.

The eye diagram is produced by displaying the received signal on an oscilloscope. The time base of the scope is triggered at a fraction of the bit rate, and it yields a sweep lasting several bit intervals. The superposition of many traces of bit intervals is shown by the oscilloscope, which is the eye diagram.

Monitoring of an eye diagram can provide a qualitative measure of performance based on the signal quality. The figure 2.9 shows the important observations of the eye diagram[8]. The width of the eye-opening represents the time interval during which the received signal can be

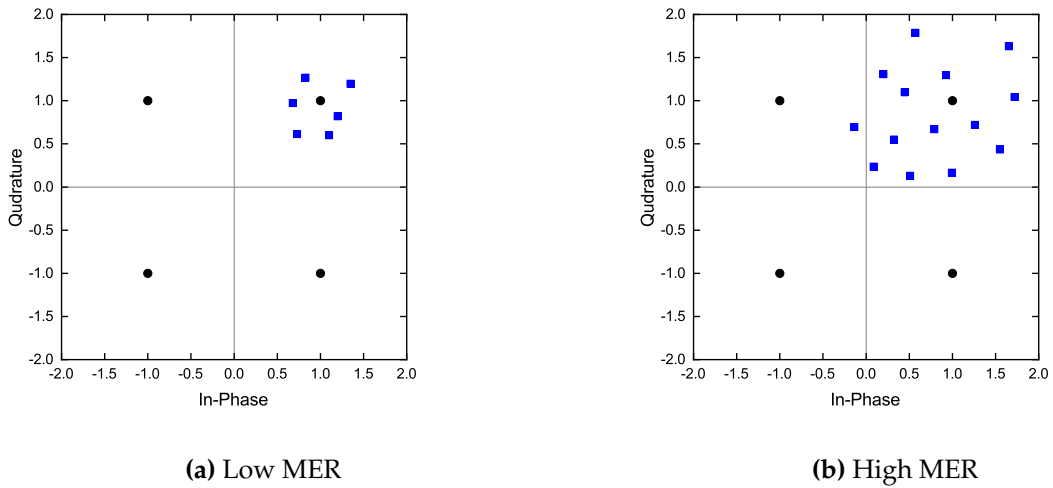


**Figure 2.8.: Schematic diagram of MER**

sampled without error from ISI. The wider the eye is opened, the better the time to sample is. When there is no ISI, an eye is opened unitively; when there is a significant amount of ISI, the eye is completely closed. In a linear system with truly random data, all the eye openings would be identical, meanwhile, asymmetries in the eye-opening generally indicate nonlinearities in the transmission channel.

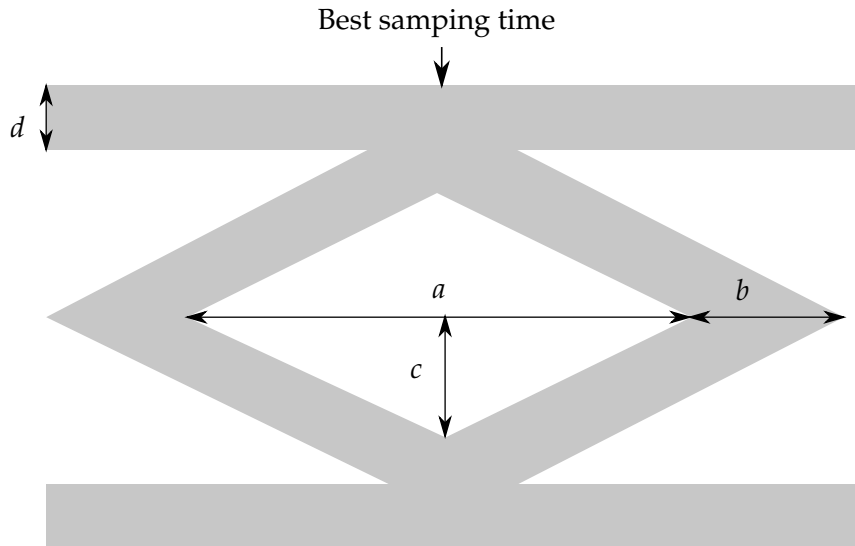


**Figure 2.9.:** Interpretation of eye diagram, *a*: Time interval for sampling, *b*: Distortion of zero crossings, *c*: Noise margin at best sampling time, *d*: Distortion at sampling instant

### 2.2.8. Noise Power Ratio

To get an accurate indication of IM distortion performance, Noise Power Ratio (NPR) is developed as an indirect indication of characterizing co-channel distortion. It has been used to measure

in-band distortion of nonlinear PAs. As Figure 2.10 shows, in this method, white noise is used to simulate the presence of many carriers of random amplitude and phase. For many systems, including those that process multicarrier signals, AWGN is a close approximation for the real-world signals [15]. This is a result of the Central Limit Theorem [16], which states that the probability distribution of a sum of a large number of random variables will approach the Gaussian distribution. The white Gaussian noise is first passed through a bandpass filter (BPF) and then a narrow band reject filter to produce a deep notch at the center of the noise pedestal as the input of the DUT. If the notch bandwidth is sufficiently narrow, power spectral density function, observed at the output within the notch position, constitutes spectral regrowth, which is the desired co-channel distortion.

Noise power ratio is therefore defined as

$$NPR(\omega_T) = \frac{S_o(\omega_T)}{S_{wd}(\omega_T)}, \quad (2.8)$$

where  $S_o(\omega_T)$  and  $S_{wd}(\omega_T)$  are the output power spectral density functions measured in the neighbor of the test window position and within that window.

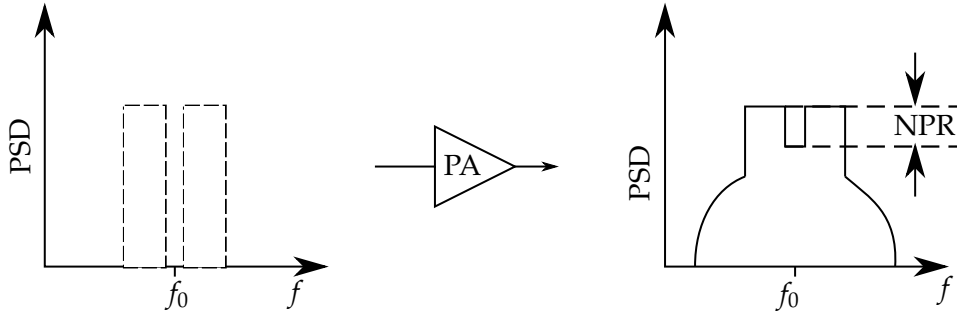


**Figure 2.10.: Definition of NPR**

Therefore, NPR represents the ratio of the output power to the effective in-band distortion power within the notch bandwidth. Despite having assumed a continuous spectrum, the NPR can also be implemented with a very large number of uncorrelated multitone signals.

### 2.2.9. Error Vector Magnitude

There are two methods to characterize the level I-Q vector error: error vector magnitude (EVM) and a quality factor called  $\rho$ -factor[12].

The error vector magnitude (EVM) is a measure to quantify the performance of a digital radio transmitter or receiver. Digital modulation requires a constellation diagram to identify each data point. Figure 2.11 shows that the ideal symbol location is often displaced by amplitude and phase error through a transmitting chain, and the measured symbol location is found in a

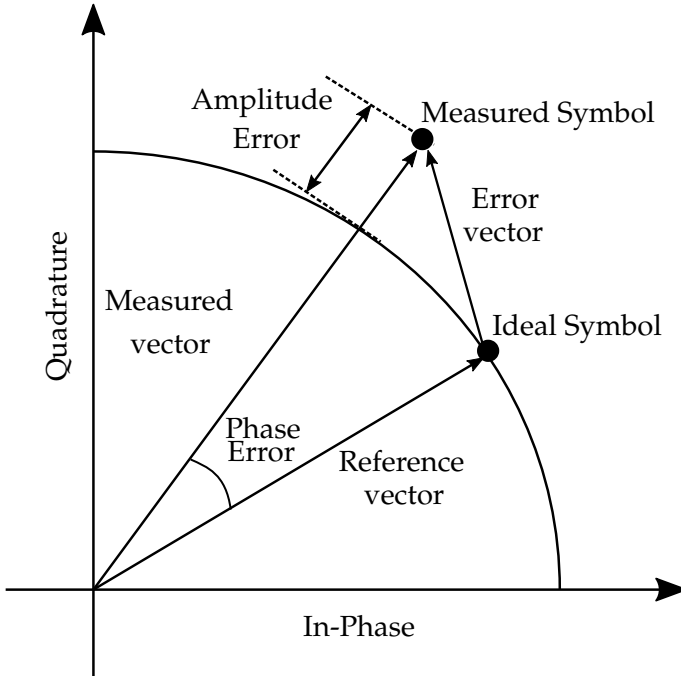


**Figure 2.11.: Vectorial Representation of Error Vector Magnitude.**

different location by an amount of an error vector. EVM expresses the difference between the expected complex voltage value of a demodulated symbol and the value of the actual received symbol.

The received symbols are plotted in a coordinate system. This coordinate system is called signal constellation, that allow to visualize modulation schemes and the effect of nonidealities on them. EVM is a quantitative measure of the impairments that corrupt the signal.

Through combination and normalization of measured symbols and ideal constellation diagram using root-mean-square, EVM can be expressed mathematically as

$$EVM = \frac{1}{P_{avg}} \frac{1}{N} \sum_{j=1}^N e_j^2 \quad (2.9)$$

where  $e_j$  denotes the magnitude of each error vector  $V_{rms}$  the root mean square power of the signal. Note that to express EVM in decibels, we compute  $10 \log(EVM)$  in terms of power amplitude [17].

EVM measurement is sensitive to amplitude and phase imbalance at the output of the complete link. It form a powerful tool for analyzing the effect of various nonidealities in the transceiver and the propagation channel. Effects such as noise, nonlinearity and ISI readily manifest themselves in both.

EVM can be related to SNR and  $\rho$  as follows

$$\begin{aligned} EVM &= \sqrt{\frac{1}{SNR}} \\ &= \sqrt{\frac{1}{\rho} - 1} \end{aligned} \tag{2.10}$$

The following calculated EVM Equations can be formulation on either in a dB scale or a percent scale.

$$EVM(dB) = 10 \log\left(\frac{ErrorVector}{ReferenceVector}\right) \tag{2.11}$$

$$EVM(%) = \sqrt{\frac{ErrorVector}{ReferenceVector}} \times 100\% \tag{2.12}$$

## 2.3. Classification of Impairments

To measure the quality of signal quantity, the constellation error of a IQ modulation signal can be expressed by EVM measurement. EVM has more information than only SNR or BER. In this report some causes of errors are introduced and classified into different categories as Figure 2.12 describes.

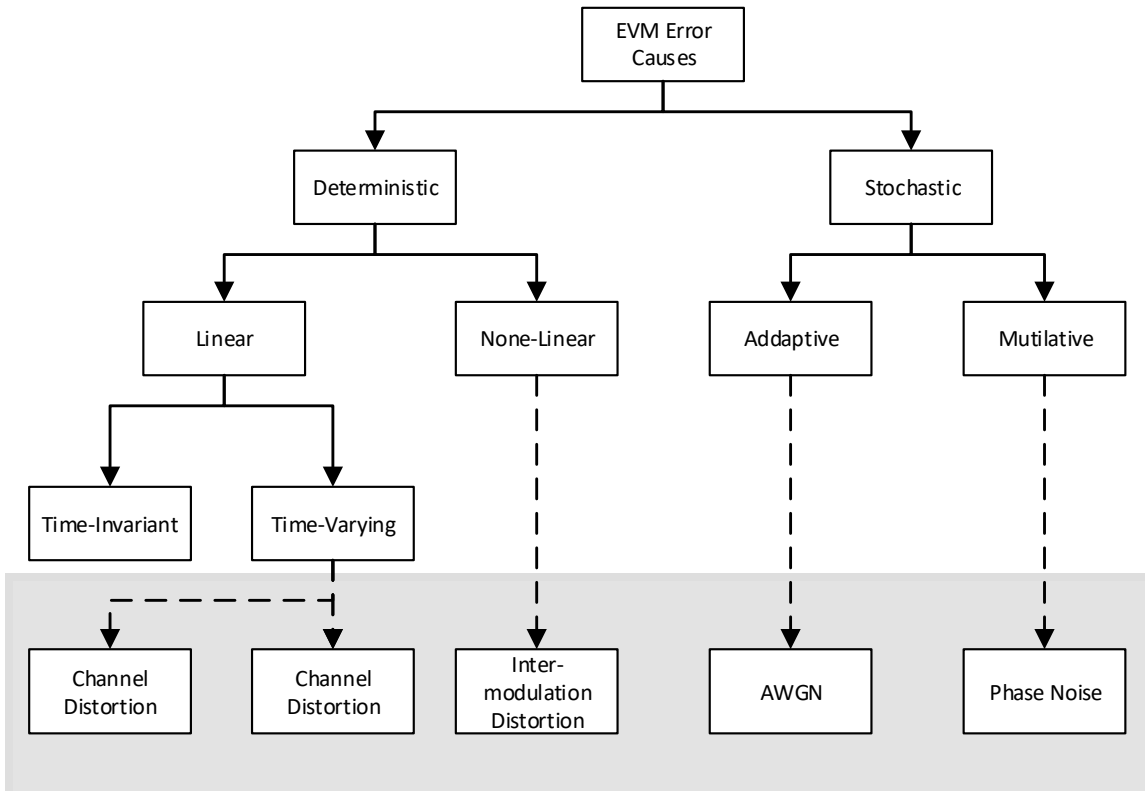


**Figure 2.12.: Classification of Analog Front-End and Channel Error Sources**

### 2.3.1. Deterministic and Stochastic System Definition

A deterministic system is a fully-defined function of the variable time. A deterministic system is a system in which there is no uncertainty with respect to its value, and every output value can be exactly determined according to the given input time.

A digital communication system is distorted not only by deterministic impairments, but also by random noise like Gaussian noise. Hence the study of stochastic system is meaningful.

A stochastic process is assigning to every outcome result  $\xi$  to a function  $x(t, \xi)$ . Thus a stochastic process is a function of  $t$  and  $\xi$ . The domain of  $\xi$  is the set of all experimental outcomes

and the domain of  $t$  is a set  $R$  of real numbers.

Given a stochastic process  $x(t)$ , if another process

$$y(t) = T[x(t)] \quad (2.13)$$

is created, whose samples are the function  $y(t, \xi_i)$ , the process  $y(t)$  can be considered as the output of a system with input  $x(t)$ . The system is completely specified in terms of the operate  $T$  as the rule of correspondence between the samples of the input  $x(t)$  and the output  $y(t)$ . Figure 2.13 shows the block Diagram of the stochastic system.

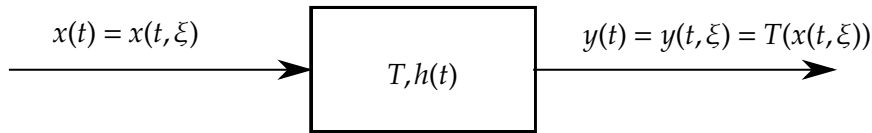


**Figure 2.13.:** Block Diagram of the Stochastic System

The system is *deterministic* if it operates only on the variable  $t$  and treats  $\xi$  as a parameter. This means if two samples  $x(t, \xi_1)$  and  $x(t, \xi_2)$  of the input are identical in  $t$ , then the corresponding samples  $y(t, \xi_1)$  and  $y(t, \xi_2)$  of the output are also identical in  $t$ . Otherwise, the system is called *stochastic* if  $T$  operates on both variables  $t$  and  $\xi$ . This means if two samples  $x(t, \xi_1)$  and  $x(t, \xi_2)$  of the input are identical in  $t$ , but  $y(t, \xi_1) \neq y(t, \xi_2)$ .

**Memoryless Systems** A system is called memoryless system if its output

$$y(t) = T[x(t)] \quad (2.14)$$

at a given time  $t = t_1$ , the output  $y(t_1)$  depends only on  $x(t_1)$  and not on any other past or future values of  $x(t)$ .

If a signal is known only in terms of statistical averages and probabilistic description, such as its mean value, mean square value, and distribution. The collection of  $k^{th}$ -order joint Cumulative Distribution Function (CDF) or Probability Density Function (PDF) are

$$\begin{aligned} F_{X(t_1), \dots, X(t_k)}(x_1, \dots, x_k) &= P[X(t_1) \leq x_1, \dots, X(t_k) \leq x_k] \\ f_{X(t_1), \dots, X(t_k)}(x_1, \dots, x_k) &= \frac{\partial^k F_{X(t_1), \dots, X(t_k)}(x_1, \dots, x_k)}{\partial x_1 \dots \partial x_k} \end{aligned} \quad (2.15)$$

The autocorrelation and autocovariance functions of the random process  $X(t)$  are as follows:

$$R_X(t_1, t_2) = E[X(t_1, t_2)] = \sum_{-\infty}^{\infty} \sum_{-\infty}^{\infty} x_1 x_2 f_{X(t_1)X(t_2)}(x_1, x_2) dx_1 dx_2 = R_X(\tau) \quad (2.16)$$

with  $\tau = t_2 - t_1$ , and

$$\begin{aligned} C_X(t_1, t_2) &= E[(X(t_1) - m_X(t_1))(X(t_2) - m_X(t_2))] \\ &= R_X(t_1, t_2) - m_X(t_1)m_X(t_2) \end{aligned} \quad (2.17)$$

To analyze deterministic time-domain signals in the frequency domain, using the Fourier transform, the PDF is

$$S_X(f) = F[R_X(\tau)] = \sum_{-\infty}^{\infty} R_X(\tau) e^{2\pi f \tau} d\tau \quad (2.18)$$

### 2.3.2. Linear and Nonlinear System

In a linear system the superposition principle is satisfied. The superposition principle is based on the additivity and homogeneity properties. A system has linearity, when the following is satisfied: if  $x_1(t) \rightarrow y_1(t)$  and  $x_2(t) \rightarrow y_2(t)$ , then exists relationships  $\alpha x_1(t) + \beta x_2(t) \rightarrow \alpha y_1(t) + \beta y_2(t)$  with  $\alpha$  and  $\beta$  as nonzero constants. Otherwise, if the superposition law is not satisfied, the system is nonlinear system.

### 2.3.3. Time-Invariant and Time-Varying System

In a time-invariant system, the input-output relationship does not change with time. This means that a time shift in the input results in a corresponding time shift in the output. A system is time-invariant if and only if the following is satisfied:

$$\text{If } x(t) \rightarrow y(t), \text{ then } x(t - \tau) \rightarrow \alpha y(t - \tau), \quad (2.19)$$

give some space between "If and x(" and ")" than and x(t")

where  $\tau$  is a real constant. A system that is not time-invariant is called a time-varying system.

In a Linear Time-Invariant (LTI) system, both linearity and time-invariance conditions must be satisfied. For LTI system, the system response of the impulse input can completely characterize the system and provide all relevant information to describe the system behavior for any input.

If the Parameters of a linear system depend on time, this system is a linear time-varying system. That means a Linear Time-Varying (LTV) system can be described as

$$y(t) = f[x(t), t] = a(t)x(t). \quad (2.20)$$

## 2.4. Deterministic Impairments

### 2.4.1. IQ Imbalance

For down-conversion progress in receiver, RF signal should be multiplied by  $\cos \omega_c t$  and  $\sin \omega_c t$  signal, in order to get I part and Q part separately. Error in the  $90^\circ$  shift circuit and mismatches between the quadrature mixers result in imbalances in the amplitudes and phases of the baseband I and Q outputs. The baseband stages themselves may also contribute significant gain and phase mismatches.

The quadrature mismatches occurs because (1) the propagation through quadrature mixers experiences mismatches, a delay mismatch of 10 ps between the two mixers translates to a phase mismatch of  $18^\circ$  at 5 GHz; (2) the quadrature phases of the LO itself are introduced.

To gain insight into the effect of I/Q imbalance, consider a QPSK signal, the input is

$$x_{in} = a \cos \omega_c t + b \sin \omega_c t \quad (2.21)$$

Because of the gain and phase mismatches shown above in the LO path,

$$\begin{aligned} x_{LO,I}(t) &= 2\left(1 + \frac{\epsilon}{2}\right) \cos\left(\omega_c t + \frac{\theta}{2}\right) \\ x_{LO,Q}(t) &= 2\left(1 - \frac{\epsilon}{2}\right) \sin\left(\omega_c t - \frac{\theta}{2}\right) \end{aligned} \quad (2.22)$$

where  $\epsilon$  and  $\theta$  represent the amplitude and phase mismatches respectively. The following baseband signals after low-pass filters are:

$$\begin{aligned} x_I(t) &= a\left(1 + \frac{\epsilon}{2}\right) \cos \frac{\theta}{2} - b\left(1 + \frac{\epsilon}{2}\right) \sin \frac{\theta}{2} \\ x_Q(t) &= -a\left(1 - \frac{\epsilon}{2}\right) \sin \frac{\theta}{2} + b\left(1 - \frac{\epsilon}{2}\right) \cos \frac{\theta}{2} \end{aligned} \quad (2.23)$$

The output  $x_I$  and  $x_Q$  contain both gain impairments and phase impairments. This impairment relies not on time and the system characters don't depend on the input, which shows it's a deterministic and time-invariant system.

If  $x_{in,1} = a_1 \cos \omega_c t + b_1 \sin \omega_c t$  and  $x_{in,2} = a_2 \cos \omega_c t + b_2 \sin \omega_c t$ , then the output of  $x_{in,1} + x_{in,2}$  are

$$\begin{aligned} &a_1 \cos \frac{\theta}{2} - b_1\left(1 + \frac{\epsilon}{2}\right) \sin \frac{\theta}{2} + a_2\left(1 + \frac{\epsilon}{2}\right) \cos \frac{\theta}{2} - b_2\left(1 + \frac{\epsilon}{2}\right) \sin \frac{\theta}{2} \\ &= (a_1 + a_2)\left(1 + \frac{\epsilon}{2}\right) \cos \frac{\theta}{2} - (b_1 + b_2)\left(1 + \frac{\epsilon}{2}\right) \sin \frac{\theta}{2} \end{aligned} \quad (2.24)$$

which is the output of the signal  $x_{in,1} + x_{in,2}$ .

Hence, IQ Imbalance is a det. LTI impairment.

Reduce this gap

### 2.4.2. Carrier Feedthrough/Leakage, IQ Offset, DC Offset

Since in a homodyne topology the downconverted band extends to zero frequency, extraneous offset voltages can corrupt the signal and saturate the following stages. Consequently, the output signal is

$$V_{out}(t) = [A(t)\cos\phi + V_{OS1}] \cos\omega_c t - [A(t)\sin\phi + V_{OS2}] \sin\omega_c t \quad (2.25)$$

where  $V_{OS1}$  and  $V_{OS2}$  denote the dc offsets from the input port of the mixers. The unconverter output therefore contains the term of the unmodulated carrier:

$$V_{out}(t) = A(t)\cos(\omega_c t + \phi) + V_{OS1} \cos\omega_c t - V_{OS2} \sin\omega_c t \quad (2.26)$$

The **carrier leakage** is quantified as

$$\text{Relative Carrier Leakage} = \frac{\sqrt{V_{OS1}^2 + V_{OS2}^2}}{\sqrt{A^2(t)}} \quad (2.27)$$

It appears to the horizontal and vertical shifts in the constellation.

If one carrier leakage pair is  $V_{OS1,1}$  and  $V_{OS2,1}$ , the other carrier leakage pair is  $V_{OS1,2}$  and  $V_{OS2,2}$ , then the sum of the outputs is

$$\begin{aligned} V_{out}(t) &= A(t)\cos(\omega_c t + \phi) + V_{OS1,1} \cos\omega_c t - V_{OS2,1} \sin\omega_c t + \\ &\quad A(t)\cos(\omega_c t + \phi) + V_{OS1,2} \cos\omega_c t - V_{OS2,2} \sin\omega_c t \\ &= 2A(t)\cos(\omega_c t + \phi) + (V_{OS1,1} + V_{OS1,2}) \cos\omega_c t - (V_{OS2,1} + V_{OS2,2}) \sin\omega_c t \end{aligned} \quad (2.28)$$

which is the output of carrier leakage pair  $V_{OS1,1} + V_{OS1,2}$  and  $V_{OS2,1} + V_{OS2,2}$  and independent of the time. Hence, Carrier Feedthrough/Leakage is a LTI impairment.

### 2.4.3. Amplitude/Phase Response depending on frequency

A LTI filter for the in-band frequencies can be simplified as its low-pass equivalent (LPE). The transfer function in the frequency domain is

$$H(\omega) = |H(\omega)| e^{-j[\theta_0(\omega) + \delta\theta]} \quad (2.29)$$

Where  $|H(\omega)|$  is the filter attenuation,  $\theta_0(\omega)$  the linear part of the phase and  $\delta\theta$  a phase offset or a phase shift in the in-band frequencies. Assuming the original I-Q signal is  $|H_s(\omega)| e^{-j\theta_s(\omega)}$ , the I-Q signal with LTI distortion is

$$X(\omega) = |H_s(\omega)H(\omega)| e^{-j[\theta_s(\omega)+\theta_0(\omega)+\delta\theta]}. \quad (2.30)$$

Too much gab, try to use the same gab between formula and text for all thesis

Above shows  $|H(\omega)|$  and  $\delta\theta$  will increase the EVM, bringing a compression and a rotation in the constellation diagram respectively. Since these effects are independent of time and the signal form, this impairment is deterministic LTI impairment.

#### 2.4.4. Multipath Propagation

One of the major challenges in wireless communications is the frequency-selectivity of the channel caused by multipath propagation, with signal echoes arriving at the receiver antenna with delays similar to, or greater than the symbol duration  $T = 1/R_s$  of the transmitted signal.

It is very likely to happen if we increase the symbol rate  $R_s = 1/T$  (to obtain higher data rates) and then, channel is no longer frequency-flat, but frequency-selective.

The multipath channel can be modelled as an FIR filter (tapped delay line) that causes (ISI). The discrete time channel impulse response with  $L + 1$  taps can be described by its  $z$ -transform as

$$H(z) = \sum_{k=0}^L h_k \cdot z^{-k} \quad (2.31)$$

or in time domain

$$y(t) = \sum_{k=0}^{\infty} a_k x(n-k) \quad (2.32)$$

The input-output relationship of  $x_1$  and  $x_2$  are

$$\begin{aligned} x_1(n) &\rightarrow \sum_{k=0}^{\infty} a_k x_1(n-k) \\ x_2(n) &\rightarrow \sum_{k=0}^{\infty} a_k x_2(n-k) \end{aligned} \quad (2.33)$$

The sum of them is

$$\sum_{k=0}^{\infty} a_k x_1(n-k) + \sum_{k=0}^{\infty} a_k x_2(n-k) = \sum_{k=0}^{\infty} a_k [x_1(n-k) + x_2(n-k)] \quad (2.34)$$

which is the output of  $x_1 + x_2$ . Besides the parameters depend not on time and input.

Hence multipath propagation is a det. LTI impairment.

#### 2.4.5. Intersymbol Interference (ISI)

A digital system consists of random sequence of ONEs and ZEROs. Each ONE represented by an ideal rectangular pulse and each ZERO by the absence of such a pulse. If this sequence is applied to a low-pass filter, the output can be obtained as the superposition of the responses to each input bit. Each bit level is corrupted by decaying tails created by previous bits. This phenomenon leads to higher error rate in the detection of random wave forms that are transmitted through band-limited channels.

The input bits applied to a pulse generator produce the following signal:

$$x(t) = \sum_{k=-\infty}^{\infty} a_k g(t - kT_b) \quad (2.35)$$

where  $g(t)$  is the basic shaping pulse with  $g(0) = 1$ , and the pulse amplitude  $a_k$  depends on the input bit.

The signal  $x(t)$  is transferred through transmitting filter  $H_T(f)$ , Channel  $H_C(f)$  added by Additive white Gaussian noise (AWGN), Receiving filter  $H_g(f)$ . The receiver signal in frequency domain is

$$R(f) = a_k G(f) H_T(f) H_C(f) H_R(f) + N(f) = A_k H(f), \quad (2.36)$$

where  $G(f)$  is the Fourier transform of the pulse  $g(t)$ . The received signal  $r(t)$  is sampled synchronously at  $t_m = mT_b$ , with  $m$  as integer values. The signal in time domain is

$$r(t_m) \sum_{k=-\infty}^{\infty} A_k h(mT_b - kT_b) + n(t_m) = A_m + \sum_{\substack{k=-\infty \\ k \neq m}}^{\infty} A_k h((m-k)T_b) + n(t_m) \quad (2.37)$$

The first term on the right-hand side of the expression above is the desired transmitted bit, and the second term represents the residual effect of all other transmitted bits on the  $m^{th}$  bit. This residual effect is called **intersymbol interference (ISI)**. The last term represents the noise sample.

The ISI term  $\sum_{\substack{k=-\infty \\ k \neq m}}^{\infty} A_k h((m-k)T_b)$  satisfied the form  $y(t) = a(t)x(t)$  mentioned above and therefore is LTV system.

#### 2.4.6. Inter-Modulation (IM) distortion

In order to study the phenomena from nonlinearity, input/output characteristic can be approximated by

$$y(t) \approx \alpha_1 x(t) + \alpha_2 x^2(t) + \alpha_3 x^3(t). \quad (2.38)$$

Therefore if two interferers at  $\omega_1$  and  $\omega_2$  are the input of a nonlinear system, the output is not harmonics of these frequencies. This phenomenon is called IM. Assuming input  $x(t) = A_1 \cos \omega_1 t + A_2 \cos \omega_2 t$ , the output according the equation above is

$$y(t) = \alpha_1 x(t) + \alpha_2 x^2(t) + \alpha_3 x^3(t). \quad (2.39)$$

Expanding the right-hand side and discarding the direct current terms, the results are the terms with the frequencies in

$$\begin{cases} \omega_1 - \omega_2 \\ 2\omega_1 - \omega_2, \quad \omega_1, \quad \omega_2, \quad 2\omega_2 - \omega_1 \\ \omega_1 + \omega_2 \\ 2\omega_1 + \omega_2, \quad 2\omega_2 + \omega_1. \end{cases} \quad (2.40)$$

It is very likely that the small desired signal at  $\omega_0$  with  $2\omega_1 - \omega_2 \approx \omega_0$ . Consequently, the IM product at  $2\omega_1 - \omega_2$  falls onto the desired channel, corrupting the signal.

The term in the frequency  $2\omega_1 - \omega_2$  is  $\frac{3\alpha_3 A_1^2 A_2}{4} \cos(2\omega_1 - \omega_2)t$ . Therefore IM is nonlinear distortion.

### 2.5. Stochastic Impairments

If it is possible, add some text here about Stochastic Impairments

#### 2.5.1. Phase Noise

An ideal oscillator produces a perfectly-periodic output of the form  $x(t) = A \cos \omega_c t$ . The zero crossings occur at exact integer multiples of  $T_s = 2\pi/\omega_c$ . In reality, however, the noise of the oscillator devices randomly perturbs the zero crossings, like  $x(t) = A \cos[\omega_c t + \phi_n(t)]$ , where  $\phi_n(t)$  is a small random phase quantity that deviates the zero crossings from integer multiples of  $T_c$ . The term  $\phi_n(t)$  is called the "phase noise". The frequency departs from  $\omega_c$  occasionally. As a consequence, the impulse is "broadened" to represent this random departure. Since  $\phi_n(t) \ll 1\text{rad}$

$$LO_{cos}(t) = A \cos[\omega_c t + \phi_n(t)] \quad (2.41)$$

After 90° delay the sin signal is

$$LO_{sin}(t) = A \sin[\omega_c t + \phi_n(t)] \quad (2.42)$$

So much gab

In the receiver front-end for down-conversion situation, referring the ideal case, the desired channel is convolved with the impulse at  $\omega_{LO}$ , yielding an IF signal at  $\omega_{IF} = \omega_{RF} - \omega_{LO}$ . However, with consideration of phase noise from LO, the convolution of the desired signal and the interferer with the noisy LO results in a broadened down-converted interferer whose noise skirt corrupts the desired IF signal. This phenomenon is called "reciprocal mixing".

The IQ signal after superposition is

$$\begin{aligned} x(t) &= I \cdot LO_{cos} - Q \cdot LO_{sin} \\ &= I \cdot A \cos[\omega_c t + \phi_n(t)] - Q \cdot A \sin[\omega_c t + \phi_n(t)] \end{aligned} \quad (2.43)$$

After the multiplication in receiver and low pass filter, the signal with I part as real part and Q part as imaginary part are

$$\begin{aligned} y(t) &= x(t) \cos(\omega_c t) + i \cdot x(t) \sin(\omega_c t) \\ &= \frac{1}{2} I e^{-i\phi} + \frac{1}{2} Q e^{-i\phi} \cdot i + \frac{1}{2} I e^{i(2\omega_c t + \phi(t))} - \frac{1}{2} Q e^{i(2\omega_c t + \phi(t))} \cdot i \\ &= \frac{I}{2} e^{-i\phi} + \frac{Q}{2} e^{-i\phi} \cdot i + \text{high frequency signal} \end{aligned} \quad (2.44)$$

The part  $e^{-i\phi}$  shows this is a phase noise and have influence on phase instead of amplitude. It is common to treat  $\phi(t)$  as a zero-mean stationary random process[18], whose variance is defined as the LO mean square phase error[13]. The description in frequency domain about phase noise is the power spectral density  $S_\phi(\omega_m)$  of the phase  $\phi(t)$ . Hence phase noise is a stochastic system.

### 2.5.2. Additive White Gaussian Noise

In communication theory it is often assumed that the transmitted signals are distorted by some noise. The most common noise is AWGN. This model is very efficient when simulate background noise or amplifier noise. AWGN is assumed to be uncorrelated with

$$E(n(t)n(t-\tau)) = \frac{N_0}{2} \delta(\tau), \quad (2.45)$$

and zero mean,  $E(n(t)) = 0$ , which means "white". With this define, the AWGN is strict sense stationary process. The AWGN channel in Figure 2.14 shows the its additivity. It is basically a

constant power spectral function, whose PDF is given by Boltzmann equation [15]:

$$[htbp]N(f) = \frac{hf}{\exp(\frac{hf}{kT}) - 1} \approx kT \quad \text{for } f < 1 \cdot 10^{12}, \quad (2.46)$$

where Boltzmann's constant is  $k = 1.38 \cdot 10^{-23} \text{ JK}^{-1}$ , Planck's constant is  $h = 6.63 \cdot 10^{-34} \text{ m kg}^2 \text{ s}^{-1}$ . The power spectral density is approximately  $-174 \text{ dBw/Hz}$ .

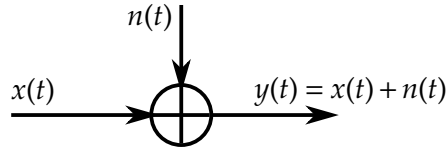


**Figure 2.14.: AWGN Channel**

If you find a nice photo about AWGN, it will be also nice to fill the page

### 3. Theory of Post Processing Methods

At this point, it is clear that channel estimation and equalization are necessary at baseband signal. This can be realized with or without knowing prior knowledge, such as channel parameters or some fixed training signals. The former is called *supervised learning* while the latter is *blind learning*. As mentioned above, since the deterministic and stochastic impairments exist together, the corresponding post methods are introduced by both supervised and blind ways. In this chapter, adaptive filters are introduced basically for deterministic impairments and some basic machine learning methods are aiming to stochastic impairments.

#### 3.1. Adaptive Filter Theory

The term filter is described for a hardware or software, whose goal is to extract information of interest from a set of noisy signal. RF signal becomes noisy by transmission through a communication channel and detected by means of noisy sensors. These noises and impairments can be both linear and nonlinear. They may be modeled by a common statistical model such as Gaussian statistical model, or random noise with unknown statistics, or may be correlated with the desired signal itself. Filtering means during the extraction of information at time  $t$  only measured data up to and including time  $t$  can be used.

The filters can be classified into linear and nonlinear. A linear filter means the output of the filter device is a linear function of the filter input. Otherwise, the filter is nonlinear. Adaptive filters are based on an approach include prior knowledge and some general models. When a priori knowledge of a dynamic process and its statistics are limited then the use of adaptive filters can offer performance improvements.

If the knowledge of the signal and noise isn't available, by using a recursive algorithm the adaptive filter can also help. If the signal and noise are stationary, the adaptive filter would converge to the optimum Wiener solution. If they are nonstationary, the adaptation rate must be faster than the rate of change.

Important features of adaptive filters contains rate of convergence, misadjustment, tracking, robustness, computational requirements, structure, numerical properties.

The baseband model of QAM system is expressed by

$$x(k) = \sum_{i=0}^{M-1} h(i)a(k-i)e^{j\phi(k)} + n(k), \quad (3.1)$$

where  $h(k)$  is the overall complex base band impulse response of the transmitter filter, channel and receiver filter. The input data sequence  $a(k)$  is assumed to be independent, identically distributed (i.i.d.) random variable with zero means.

### 3.1.1. Linear Adaptive Filters

For linear impairments, if the  $n$ th symbol  $\sum b_n u(t - nT)$  is to be sent, the received waveform in  $z$ -domain is a linear combination of

$$X(z) = \sum_{k=-\infty}^{\infty} b_k z^{-k} U(z). \quad (3.2)$$

If the received waveform is filtered with a FIR filter

$$H(z) = \frac{1}{\sum_{k=-\infty}^{\infty} b_k z^{-k}}, \quad (3.3)$$

this linear impairment is fully removed. In order to complete the channel coefficient  $b_n$ , a transversal structure is used with recursive algorithm.

Transversal structure is very successfully employed for practical systems. It is similar to the linear FIR filter structure as Figure 3.1.

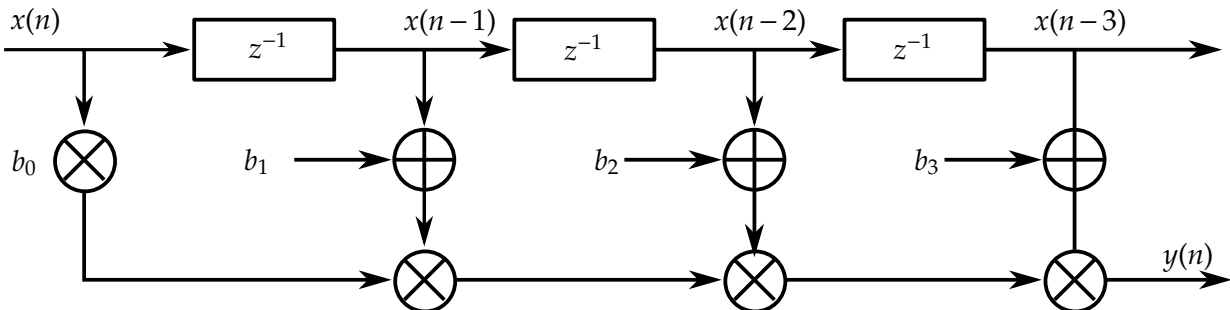


Figure 3.1.: FIR Transversal Structure

The model can be described as

$$y[n] = \sum_{k=0}^M b(k)x(n-k) \quad (3.4)$$

In this model,  $b[n]$  is the weights of different delay paths as the filter coefficients. This filter can be made into an adaptive filter by calculating the coefficients  $b[n]$  progressively at each time step.

### 3.1.2. Supervised Adaptive Filter Algorithm

Supervised adaptive filter means in order to get channel coefficient  $a_n$ , a series of ideal data  $d_n$  should first be given as priori knowledge of reference.

One of the mostly well-used objective function adaptive filter is the **mean-square error (MSE)**, defined as

$$\xi = E[e^2(k)] = E[d^2(k) - 2d(k)y(k) + y^2(k)], \quad (3.5)$$

where  $d(n)$  is the reference signal.

For the FIR transversal structure above, the output signal is composed by a linear combination of inputs as

$$y(k) = \sum_{i=0}^N w_i(k)x_i(k) = \mathbf{w}^T(k)\mathbf{x}(k), \quad (3.6)$$

where  $\mathbf{x}(k) = [x(k)x(k-1)\dots x(k-N)]^T$  is the input vector with a tapped-delay line, and  $\mathbf{w}(k) = [w_0(k)w_1(k)\dots w_N(k)]^T$  as weight factor of each tap.

Hence the MSE function in a stationary environment is given by

$$\xi = E[d^2(k)] - 2\mathbf{w}^T \mathbf{p} + \mathbf{w}^T \mathbf{R} \mathbf{w}, \quad (3.7)$$

where  $\mathbf{p} = E(s[n]\mathbf{x}[n])$  is the cross-correlation vector between the desired and input signals, and  $\mathbf{R} = E(\mathbf{x}[n]\mathbf{x}[n]^T)$  is the input signal correlation matrix.

The gradient vector of MSE function is given by

$$\mathbf{g}_w = -2\mathbf{p} + 2\mathbf{R}\mathbf{w}. \quad (3.8)$$

By equating the gradient vector  $\mathbf{g}_w$  to zero, the solution is

$$\mathbf{w}_o = \mathbf{R}^{-1}\mathbf{p}. \quad (3.9)$$

This solution is called Wiener solution. However, in practice, accurate estimations of correlation matrix  $\mathbf{R}$  and cross-correlation vector  $\mathbf{p}$  are not available. If the input  $\mathbf{x}(n)$  and the reference signal  $d(n)$  are ergodic, it is popular performed by most adaptive algorithms to use time averages to estimate  $\mathbf{R}$  and  $\mathbf{p}$ .

The estimation is

$$\begin{aligned}\hat{s}(n) &= \mathbf{h}^T \mathbf{x} \\ &= \mathbf{p}^T \mathbf{R}^{-1} \mathbf{x} \\ &= E[s(n)\mathbf{x}^T(n)]E[\mathbf{x}(n) \cdot \mathbf{x}^T(n)]^{-1}\mathbf{x}(n)\end{aligned}\quad (3.10)$$

### 3.1.2.1. Least-Mean-Square (LMS) Algorithm

The least-mean-square (LMS) is a search algorithm by using the gradient vector computation in order to approach the target point iteratively. The LMS algorithm is widely used in various adaptive filters. The advantages of LMS in Wiener filter are low computational complexity, unbiased convergence in the mean to the Wiener solution and stable behavior.

As mentioned above, the optimal Wiener solution is  $\mathbf{w}_o = \mathbf{R}^{-1}\mathbf{p}$ . If good estimates of  $\mathbf{R}$  and  $\mathbf{p}$  denoted by  $\hat{\mathbf{R}}(k)$  and  $\hat{\mathbf{p}}(k)$  are available, a steepest-descent-based algorithm can be used as

$$\begin{aligned}\mathbf{w}(k+1) &= \mathbf{w}(k) - \mu \hat{\mathbf{g}}_{\mathbf{w}}(k) \\ &= \mathbf{w}(k) + 2\mu(\hat{\mathbf{p}}(k) - \hat{\mathbf{R}}(k)\mathbf{w}(k))\end{aligned}\quad (3.11)$$

for  $k = 0, 1, 2, \dots$ , where  $\hat{\mathbf{g}}_{\mathbf{w}}(k)$  is an estimate of the gradient vector (equation 3.8) of the objective function with respect to  $\mathbf{w}$ .

One widely used estimations of  $\mathbf{R}$  and  $\mathbf{p}$  are as follows:

$$\begin{aligned}\hat{\mathbf{R}}(k) &= \mathbf{x}(k)\mathbf{x}^T(k) \\ \hat{\mathbf{p}}(k) &= d(k)\mathbf{x}(k)\end{aligned}\quad (3.12)$$

The resulting gradient estimate  $\hat{\mathbf{g}}_{\mathbf{w}}(k)$  is expressed by

$$\begin{aligned}\hat{\mathbf{g}}_{\mathbf{w}}(k) &= 2\mathbf{x}(k)(-d(k) + \mathbf{x}^T(k)\mathbf{w}(k)) \\ &= -2e(k)\mathbf{x}(k)\end{aligned}\quad (3.13)$$

Then we get **LMS algorithm** :

First as initialization set  $\mathbf{x}(0) = \mathbf{w}(0) = [0 \ 0 \ \dots \ 0]^T$ .

Then for  $k = 0, 1, 2, \dots$

$$\begin{aligned}e(k) &= d(k) - \mathbf{x}^T(k)\mathbf{w}(k) \\ \mathbf{w}(k+1) &= \mathbf{w}(k) + 2\mu e(k)\mathbf{x}(k)\end{aligned}\quad (3.14)$$

### 3.1.2.2. Recursive Least-Squares (RLS) Algorithm

In LMS algorithm, for each iteration only the information of time interval  $n = k$  is used. However, if not only last point, but also several previous points are used together, the convergence speed may be much faster. This idea is recursive least-squares (RLS) algorithm.

The RLS algorithms performs well with its fast convergence even when the eigenvalue spread of the input signal correlation matrix is large. Hence it has excellent performance for estimating the time-varying parameters. On the other hand, all these advantages take the cost of an increased computational complexity and larger possibility of unstable than LMS-based algorithm.

Simillar to LMS, assume the input signal information vector at a given instant  $k$  is given by

$$\mathbf{x}(k) = [x(k) \quad x(k-1) \dots x(k-N)]^T \quad (3.15)$$

where  $N$  is the order of the filter. The weight coefficients  $w_j(k)$ , for  $j = 0, 1, \dots, N$ , the objective function is given by

$$\begin{aligned} \xi^d(k) &= \sum_{i=0}^k \lambda^{k-i} \epsilon^2(i) \\ &= \sum_{i=0}^k \lambda^{k-i} [d(i) - \mathbf{x}^T(i) \mathbf{w}(k)]^2 \end{aligned} \quad (3.16)$$

where  $\mathbf{w}(k) = [w_0(k) \quad w_1(k) \dots w_N(k)]^T$  is the adaptive-filter coefficient vector and  $\epsilon(i)$  is the posteriori output error at instant  $i$ . The parameter  $\lambda$  is an exponential weighting factor called forgetting factor that satisfies  $0 < \lambda \leq 1$ . The information far in the past has lower weight on the coefficient updating.

As we can observe, each error is the difference between the desired signal and the filter estimation using the most recent coefficients  $\mathbf{w}(k)$ . Because in each iteration the coefficient  $\mathbf{w}(k)$  is better than previous  $\mathbf{w}$ , the new error uses posterori information and the algorithm consists of faster convergence.

By differentiating  $\xi^d(k)$  with respect to  $\mathbf{w}(k)$ , it is

$$\frac{\partial \xi^d(k)}{\partial \mathbf{w}(k)} = -2 \sum_{i=0}^k \lambda^{k-i} \mathbf{x}(i) [d(i) - \mathbf{x}^T(i) \mathbf{w}(k)] \quad (3.17)$$

By equating  $\frac{\partial \xi^d(k)}{\partial \mathbf{w}(k)}$  to zero, the optimal coefficient vector  $\mathbf{w}(k)$  is given by

$$\begin{aligned}\mathbf{w}(k) &= \left[ \sum_{i=0}^k \lambda^{k-i} \mathbf{x}(i) \mathbf{x}^T(i) \right]^{-1} \sum_{i=0}^k \lambda^{k-i} \mathbf{x}(i) d(i) \\ &= \mathbf{R}_D^{-1}(k) \mathbf{p}_D(k)\end{aligned}\quad (3.18)$$

where  $\mathbf{R}_D(k)$  and  $\mathbf{p}_D(k)$  are called the deterministic correlation matrix of the input signal and the deterministic cross-correlation vector between the input and desired signals.

Then we get **Conventional RLS algorithm** :

First as initialization set  $\mathbf{S}_D(-1) = \mathbf{R}_D^{-1}(-1) = \delta \mathbf{I}$  where  $\delta$  can be the inverse of the input signal power estimate

$$\mathbf{p}_D(-1) = \mathbf{x}(-1) = [0 \ 0 \ \dots \ 0]^T$$

Then for  $k = 0, 1, 2, \dots$

$$\begin{aligned}\mathbf{S}_D(k) &= \mathbf{R}_D^{-1}(k) = \frac{1}{\lambda} [\mathbf{S}_D(k-1) - \frac{\mathbf{S}_D(k-1) \mathbf{x}(k) \mathbf{x}^T(k) \mathbf{S}_D(k-1)}{\lambda + \mathbf{x}^T(k) \mathbf{S}_D(k-1) \mathbf{x}(k)}] \\ \mathbf{p}_D(k) &= \lambda \mathbf{p}_D(k-1) + d(k) \mathbf{x}(k) \\ \mathbf{w}(k) &= \mathbf{S}_D(k) \mathbf{p}_D(k)\end{aligned}\quad (3.19)$$

### 3.1.3. Blind Adaptive Filtering

For supervised adaptive filter mentioned above, a series of ideal or required data is required to generate the error signal. However, there are lots of applications where the reference signals are not available. Furthermore, if the training data is not required, the pressure of transformation could be reduced and higher transformation speed can be reached. This kind of adaptive filter, which doesn't utilize reference signal is called unsupervised adaptive filter or blind adaptive filter. Since blind adaptive filters don't demand training data during learning, the algorithms are specifically suitable for an unknown environment.

#### 3.1.3.1. Circularity-Based Approach

One of the major impairments affecting direct conversion receivers is the imbalance between the received signal's in-phase and quadrature components. Rather than improving the front-end, analog hardware, it is more cost effective to tolerate a certain level of IQ imbalance and then implement compensation methods. A circularity-based blind compensation algorithm is used as the basis for the I/Q Imbalance Compensator [19].

This suggests the compensator structure as shown in which discrete-time notation is used to express

the variables. The compensated signal is expressed as

$$y(n) = x(n) + \mathbf{w}^T \cdot \mathbf{x}^*(n). \quad (3.20)$$

The cost function of circularity based approach is

$$J = E[\mathbf{y}(n)y(n)] = 0, \quad (3.21)$$

since the output should be "proper" (as Anttila wrote) or irrelevant.

A simple algorithm approaching the cost function above is

$$\begin{aligned} y(n) &= x(n) + \mathbf{w}^T(n)\mathbf{x}^*(n) \\ \mathbf{w}(n+1) &= \mathbf{w}(n) - \mathbf{M}\mathbf{y}(n)y(n), \end{aligned} \quad (3.22)$$

where output vector  $\mathbf{y}(n) = [y(n), y(n-1), \dots, y(n-N+1)]^T$  and step-size matrix  $\mathbf{M} = \text{diag}(\mu_1, \mu_2, \dots, \mu_N)$ .

### 3.1.3.2. $p$ - Constant-Modulus Algorithm!

The CMA, proposed by Godard in 1980[20], is the most popular algorithm for blind adaptive filter of QAM communication.

The basic idea is to minimize the distance between the modulus of the equalizer output and some constant values[21]. In this way a reference signal is not required. These constant values, normally denoted by  $R_p$ , express the modulus of constellation symbols. The earlier blind algorithm was addressed the case of Pulse Amplitude Modulation (PAM). This method was later developed with objective function to apply to the case of Quadrature Amplitude Modulation (QAM)[22].

The cost function of CMA is expressed by

$$J(k) = E[(|y(k)|^p - R_p)^2], \quad (3.23)$$

where  $E[\bullet]$  indicates statistical expectation. Employing a stochastic gradient of cost function  $J(k)$  with respect to the weights vector  $\mathbf{w}(k)$ , the iteration function is adapted by

$$\begin{aligned} w(k+1) &= w(k) - \mu \cdot \nabla J(k) \\ &= w(k) - \mu y(k) |y(k)|^{p-2} (|y(k)|^p - R_p) \mathbf{x}^*(k), \end{aligned} \quad (3.24)$$

where  $\mu$  is the step-size parameter and  $*$  denotes complex conjugation.  $R_p$  is the constant modulus depending only on the input data as[20]

$$R_p = \frac{E[|a(k)|^{2p}]}{E[|a(k)|^p]}. \quad (3.25)$$

Godard proved that this method is also suitable for rectangular QAM constellation although it's non-constant modulus.

### 3.2. Machine Learning Method

The demodulation process is basically a pattern classification problem, which is already extensively discussed in the Machine Learning (ML) area. ML plays a role in various areas (exp. data mining, pattern recognition and classification, image processing) as a powerful tool with interdisciplinary. Lately, several classical ML methods are also amplified in demodulation process, such as  $k$ -NN Method [23], SVM Method [24], MLE Method.

Since all these Methods are supervised ML, a prefixed training data is necessary for further processing. Specifically for 16-QAM, various constellation points are regarded as 16 classes of data, where each received data point can be represented as a two-dimensional vector ( $I(\mathbf{x}), Q(\mathbf{x})$ ). The correct demodulation results are already known as a reference. The whole data points are divided into two parts: a small amount with label  $y(\mathbf{x})$  as training data set and the rest as the test data set. The basic idea is: With training data and corresponding labels as known information, the test set is classified to modulation points. Then compare the classify results with correct reference and calculate BER.

All ML Methods mentioned above will be discussed and applied to support demodulation process in phase noise distortion.

#### 3.2.1. KNN Method

As a classification algorithm, KNN is used to classify the received signals to different constellations. It is straightforward and effective, especially for large data with low dimensions [23]. Hence, KNN is particularly suitable for demodulation if it improves the appearance.

To begin with, the distances of each point in the test set ( $\mathbf{x}_i$ ) to every point in the train set  $\mathbf{x}_j$  need to be calculated as

$$d(\mathbf{x}_i, \mathbf{x}_j) = \sqrt{(I(\mathbf{x}_i) - I(\mathbf{x}_j))^2 + (Q(\mathbf{x}_i) - Q(\mathbf{x}_j))^2}. \quad (3.26)$$

After the distances sorted in ascending order,  $k$  nearest training data points are determined as  $N_k(\mathbf{x}_i)$ . The majority of these  $k$  labels is regarded as the predicted label for  $\mathbf{x}_i$ :

$$f_{KNN}(\mathbf{x}_i) = \arg \max_{l \in \mathbf{L}} \sum_{i \in N_k(\mathbf{x}_i)} \delta(l, l_i), \quad (3.27)$$

where  $\delta(l, l_i) = 1$  if  $l = l_i$  and  $\delta(l, l_i) = 0$  if  $l \neq l_i$ ,  $\mathbf{L} = \{1, 2, \dots, 16\}$  is the label set.

Furthermore, in order to get higher accuracy, the closer points in train set  $\mathbf{x}_j$  should have greater weights. With a weight vector  $\omega_j = 1/d(\mathbf{x}_i, \mathbf{x}_j)^2$  based on distance  $d(\mathbf{x}_i, \mathbf{x}_j)$ , a distance weighted KNN method is proposed as:

$$f_{\omega KNN}(\mathbf{x}_i) = \arg \max_{l \in \mathbf{L}} \sum_{i \in N_k(\mathbf{x}_i)} \omega_i \delta(l, l_i). \quad (3.28)$$

KNN is one of the most intuitive ML method. In the next chapter, the simulation results will be discussed and compared with other methods.

so much gab

### 3.2.2. SVM Method

SVM is another straightforward and well-implicated decision machine. Basic SVM is a two-class classification with linear models of the form

$$y(\mathbf{x}) = \mathbf{w}^T \phi(\mathbf{x}) + b, \quad (3.29)$$

where  $\phi(\mathbf{x})$  denotes a fixed feature-space transformation, and  $b$  is the bias parameter. Assume that train data set as  $N$  input vectors  $\mathbf{x}_1, \mathbf{x}_2, \dots, \mathbf{x}_N$  with corresponding labels  $t_1, t_2, \dots, t_N$  is linearly separable in feature space, where  $t_n \in \{-1, 1\}$ , and new data points  $\mathbf{x}$  are classified based on the sign of  $y(\mathbf{x})$ . According to the definition (linear separable) there exists at least one weight parameters vector  $\mathbf{w}$  and one bias parameter vector  $b$  such that  $y(\mathbf{x}) > 0$  for all  $\{\mathbf{x}_i | t_i = 1\}$  and  $y(\mathbf{x}) < 0$  for all  $\{\mathbf{x}_i | t_i = -1\}$ .

The SVM approaches this two-class classification problem with the concept *margin*, which is defined as the smallest distance between decision boundary and any samples like Figure 3.2.

Normally there exist several solutions for  $\mathbf{w}$  and  $b$ . By the definition of margin, the best solution is decided. According to [25], in SVM the decision boundary is chosen to maximize the margin. In a

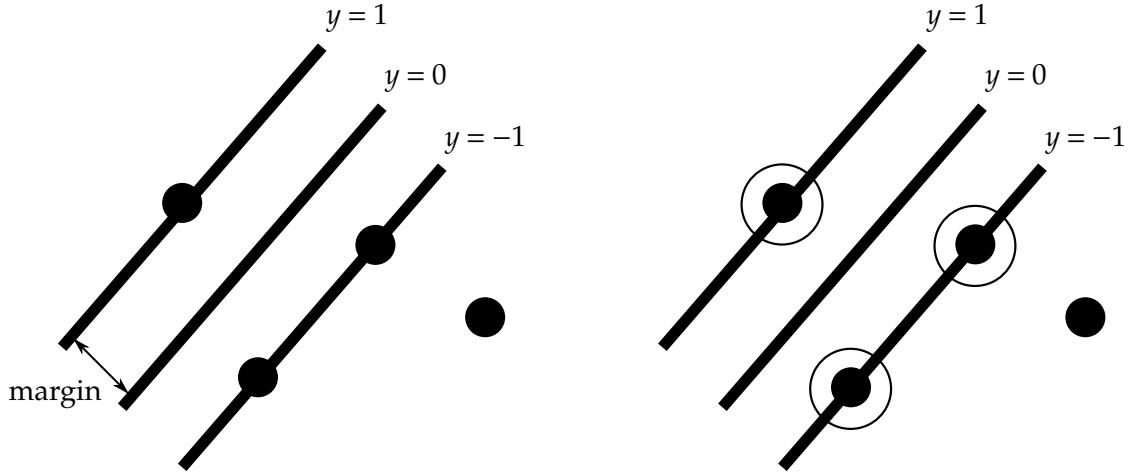


**Figure 3.2.:** Basic SVM Concept with support vectors in circles

hyperplane the distance of a point  $\mathbf{x}$  from a hyperplane  $y(\mathbf{x}) = 0$  is given by

$$\text{distance}(\mathbf{x}, y) = \frac{|y(\mathbf{x})|}{\|\mathbf{w}\|}. \quad (3.30)$$

Thus the maximum margin solution is found by solving

$$\arg \max_{\mathbf{w}, b} \left\{ \frac{1}{\|\mathbf{w}\|} \min_n [t_n (\mathbf{w}^T \phi(\mathbf{x}_n) + b)] \right\} \quad (3.31)$$

so much gab

Since scaling makes no influence on solution[25], in order to simply the problem,  $(\mathbf{w}, b)$  is scaled to insure

$$\min_{\mathbf{w}, b} |\mathbf{w}^T \mathbf{x} + b| = 1. \quad (3.32)$$

Then the original problem 3.31 is transformed as

$$\begin{aligned} & \underset{\mathbf{w}, b}{\operatorname{argmin}} \frac{1}{2} \mathbf{w}^T \mathbf{w} \\ & \text{s.t. } y_i (\mathbf{w}^T \mathbf{x}_i + b) \geq 1, \quad i = 1, 2, \dots, m. \end{aligned} \quad (3.33)$$

After that Lagrange Function, Dual Problem and Karush-Kuhn-Tucker(KKT) conditions are introduced[26], this problem becomes a convex linear optimization problem.

Until here, it is assumed that there exists a hyperplane, which can separate the training points with different labels. However, various tasks don't satisfy this condition. SVM solved the limitation of linear separation through so-called *kernel trick*.

Since original vector space  $\mathbb{R}^d$  is linear inseparable, SVM uses a mapping relation  $\phi : \mathbb{R}^d \rightarrow \mathbb{R}^{\hat{d}}$

to ensure the training points linear separable in new vector space  $\mathbb{R}^{\hat{d}}$  like Figure 3.3. According to Vapnik [27] the dimension number  $\hat{d}$  must exist if  $d$  is a limited number.

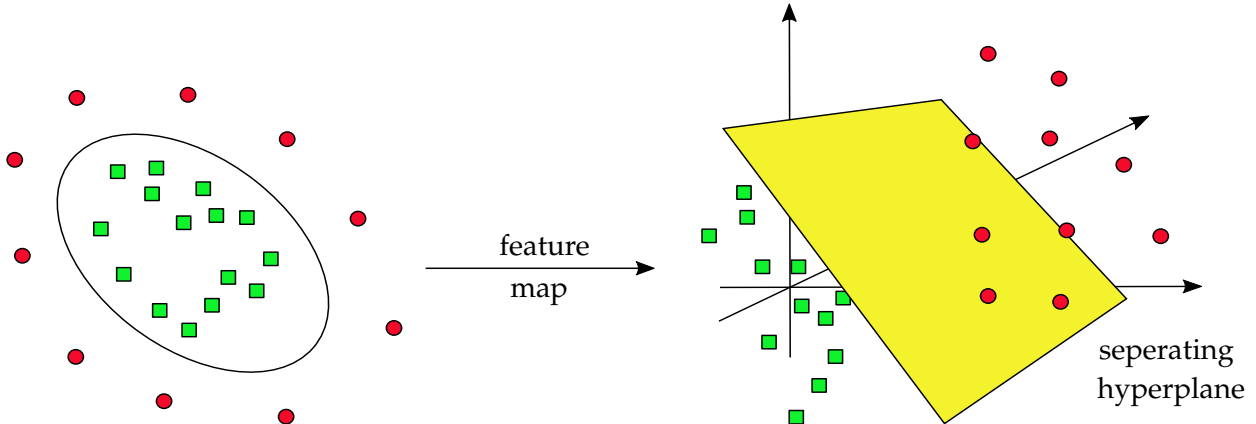


**Figure 3.3.:** Linear inseparable points in low dimension (2-D) become separable in higher dimensions (3-D)

Since in SVM inner product is repeatedly used(dual problem), kernel trick converges mapping and inner product to one step, in order to reduce the computing complexity from  $O(\hat{d})$  to  $O(d)$  at the same time.

Finally, the algorithm of SVM is as following:

- **Given**
  - training samples  $\mathbf{x}_i$  and labels  $y_i$
- **Parameter**
  - kernel function  $K(\mathbf{x}_m, \mathbf{x}_n)$
- **Training**
  - compute  $\mathbf{Q} = [Q_{mn}]$  with  $Q_{mn} = y_m y_n K(\mathbf{x}_m, \mathbf{x}_n)$
  - compute  $\alpha$  by solving the convex quadratic problem  $\min_{\alpha} \frac{1}{2} \alpha^T \mathbf{Q} \alpha - \mathbf{1}^T \alpha$
  - determine the index set  $SV = n | \alpha_n > 0$  of support vectors
  - compute  $w_0 = \frac{1}{|SV|} (\sum_{n \in SV} y_n - \sum_{m \in SV} \sum_{n \in SV} \alpha_m y_n Q_{mn})$
- **Classification**
  - calculate the discriminant function  $f(\mathbf{x}) = \sum_{n \in SV} \alpha_n y_n K(\mathbf{x}_n, \mathbf{x}) + w_0$
  - estimate the class  $\hat{y}(\mathbf{x}) = \text{sgn}(f(\mathbf{x}))$



So much gab

## 4. Filters Design and Simulation Results

This chapter is under the assumption that the received signal suffers from medium deterministic and stochastic impairments. The corresponding parameters are introduced in the first section. The algorithms for channel equalizers including adaptive filters and ML methods are implemented in MATLAB. Original received signals are generated in Keysight Advanced Design System (ADS) and Ptolemy co-simulation. The performances are compared and discussed based on EVM and BER. At last, through discussion of computational complexity and progress speed, the possibility of applying is demonstrated.

In higher order modulation schemes, like 64-QAM, the distance between the constellation points is less so for the same amount of distortion. Therefore, higher order modulation schemes demand better EVM in comparison to lower order modulation, like Quadrature Phase-Shift Keying (QPSK). At this medium impairments, three signal constellations are considered: 4-QAM, 16-QAM, 64-QAM.

### 4.1. Received Signal Generator

ADS is the world's leading electronic design automation software for RF, microwave, high speed digital, and power electronics applications[28]. With an easy-used interface, received signal w/o various impairments are generated in ADS.

The relative parameters in Simulation are in Table 4.1.

Transmitter	Modulation type	QPSK, 16-QAM, 64-QAM
	Modulation type for the reference signal	QPSK <span style="color:red">This is not clear, you are using 3 modulation but only one reference</span>
	No. of frames per run	50
	No. of symbols per frame	1000
Channel	SNR	20 to 30
	IQ Imbalance	3 dB, 3°
	Multipath	5 dB
	Phase Noise	-40 dBc/Hz, $f_{\text{offset}} = 10 \text{ Hz}$
Receiver	Adaptation step size	0.08
	No. of filter taps	6
	Adaptive methods	LMS, RMS, CMA, kNN, SVM,

Table 4.1.: Simulation Condition

## 4.2. Convergence Analysis

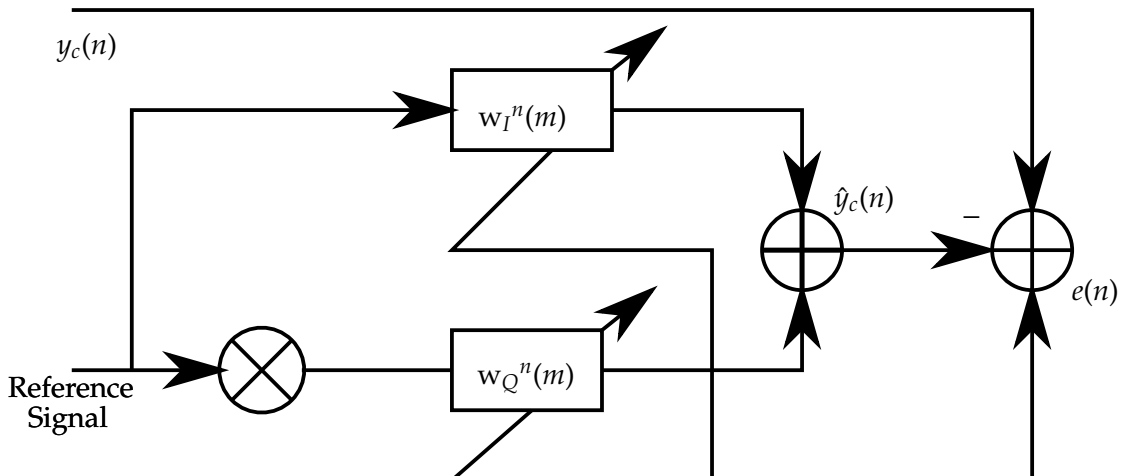
Convergence speed and results are the main part of adaptive filter performance. Hence, in this section, we will discuss it in detail. Before using various adaptive filters, we remove kinds of offset in the first place. through simple data processing. We remove the constellation center of received data and proceed normalization through the formula

$$x_{\text{train}} = \frac{x_{\text{train}} - x_{\text{mean}} \cdot \mathbf{1}}{x_{\text{mean}}}, \quad (4.1)$$

where  $\mathbf{x}_{\text{train}}$  is received training data set (column vector),  $x_{\text{mean}}$  is mean value of training data and  $\mathbf{1}$  is a column vector with  $\mathbf{x}_{\text{train}}$  size.

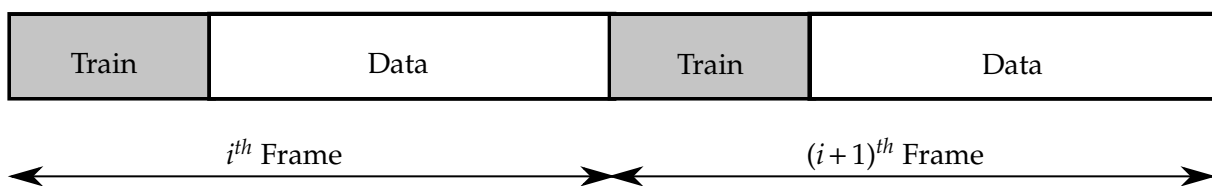
#### 4.2.1. Supervised Adaptive Compensator: LMS and RMS

This section presents the adaptive method for IQ Imbalance and multipath propagation impairment. In this method, parameters of both impairments are estimated according to the functional block diagram of Figure 4.1.



**Figure 4.1.:** Supervised Adaptive Compensator

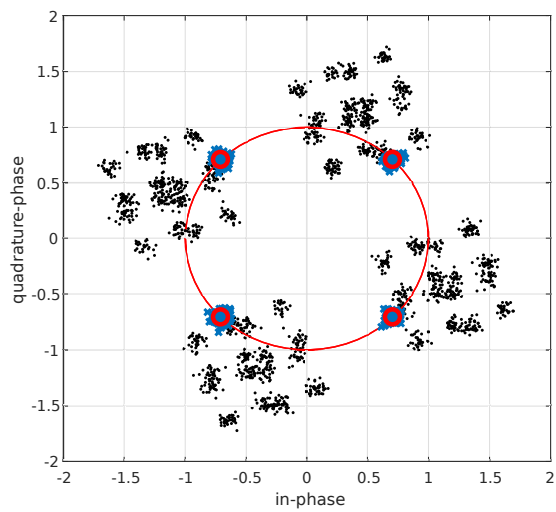
Since *a priori* knowledge is required, the transmit data is arranged in a frame structure as shown in Figure 4.2. Each frame contains training symbols followed by data symbols.



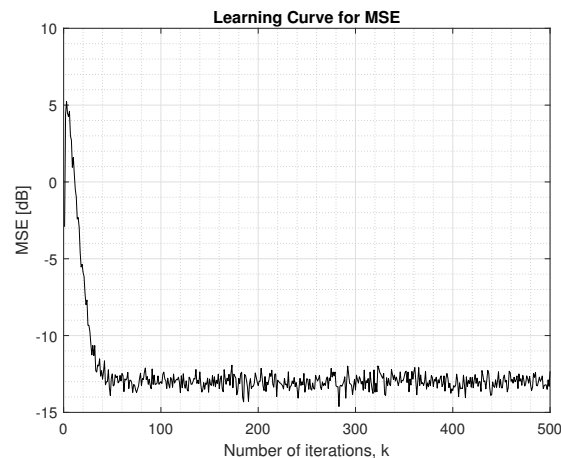
**Figure 4.2.: A frame structure that contains reference training signal and transmitted data**

Figure 4.3a shows the constellation results scattered from the original location (the red circles) due to the IQ imbalance and channel distortion. The black points are the constellation of the received

signal without constellation, while the blue points are the constellation after Compensator with LMS algorithms. From Figure 4.3b shows the convergence speed in this compensation. After about 50 times iterations the learning line stays stable, which means the weight vector  $w(x)$  is convergence converged and the algorithms can't do better. The distortion observed in constellations of the adaptive LMS compensation is much less than that of untreated data, which has been reflected later in the EVM and SER results.



(a) Constellation Graph



(b) Learning / Convergence Line

**Figure 4.3.: Equalizer with LMS Adaptive Filter for 4-QAM**

The EVM structures for supervised adaptive filters LMS and RMS have been shown in Figure 4.4. It should be noted that the EVM and SER performances have been shown for a 64-QAM modulation scheme only. The legend 'Uncompensated' refers to the received data that has not treated with any correction or detection method. The term 'Ideal' refers to the ideal case where the received signal  $x$  doesn't have any IQ or channel distortion. The only distortion for the ideal case is the AWGN.

The results show that supervised adaptive filter including LMS and RMS work really satisfying. With limited taps and iterations, the distortion for IQ imbalance and multipath channel distortions are almost faded away. In  $Eb/N_0 = 30$  dB, the EVM decreased from about 18% to 2%, which is already very close to the ideal signal with 2%.

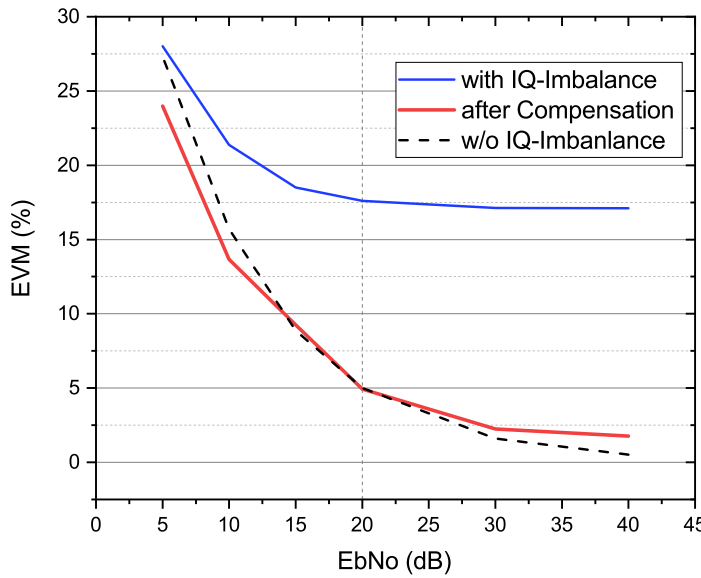


**Figure 4.4.:  $Eb/N_0$  w/o RMS Adaptive Filter for 4-QAM**

Specifically, RMS algorithms is tested more detailed as Figure 4.5 in various Gain Imbalances ( in dB ) and Phase Imbalance ( in degree ). Signal is generated in ADS software with given parameters Gain Imbalance from 0 decibel to 6dB and Phase Imbalance from 0 degree to 5 degree. The EVM value shows more sensitive in Gain Imbalance than Phase Imbalance. In this figure RMS makes a satisfying performance in different mesh points of Gain Imbalance and Phase Imbalance. IQ imbalance and channel distortion are compensated almost completely.

#### 4.2.2. Blind Adaptive Compensator: CMA and modified CMA

As described in Chapter 3, the CMA algorithm relies neither on the symbol decisions nor on a training sequence. This algorithm operates blindly based on the statistical property that the average power of received signal  $P(x)$  should be constant. Therefore, the CMA is not suitable for M-QAM if  $M > 4$ , since such modulations do not satisfy a constant power property any more. Savory [29] shown that the error function has a non zero optimum minimum. Since the error tends to be non zero, the stochastic gradient descent method works not as we hope and therefore degrading the performance.

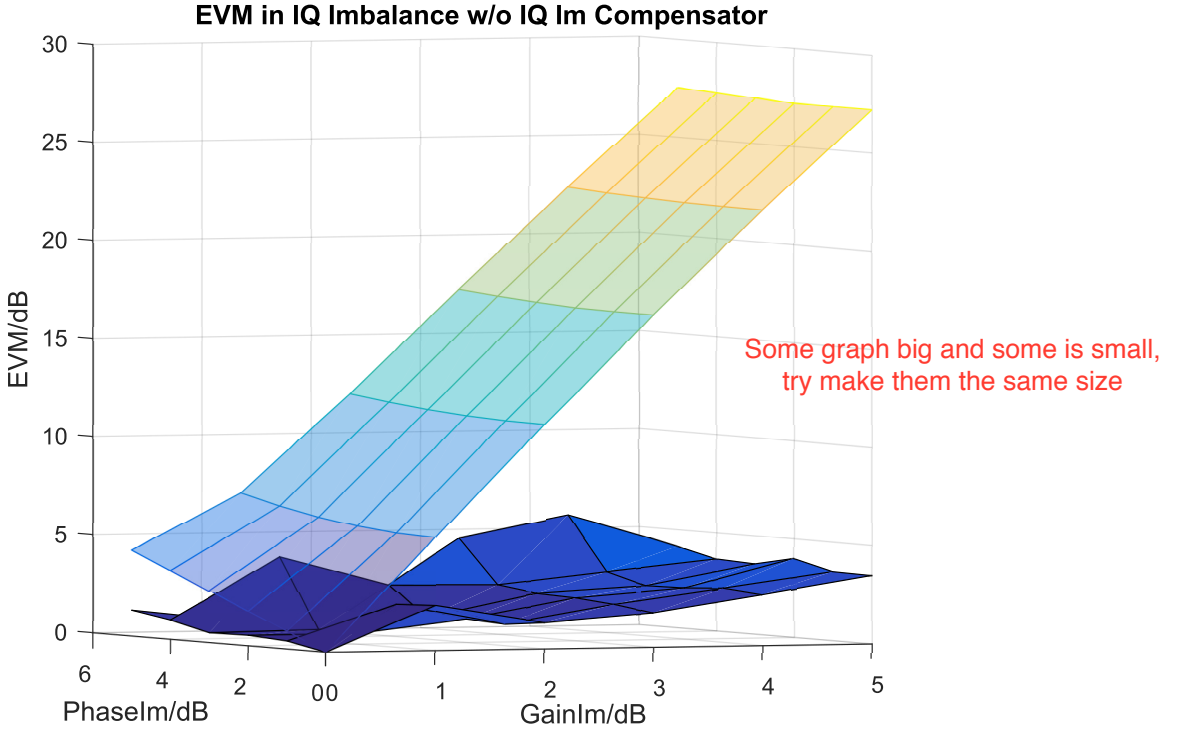
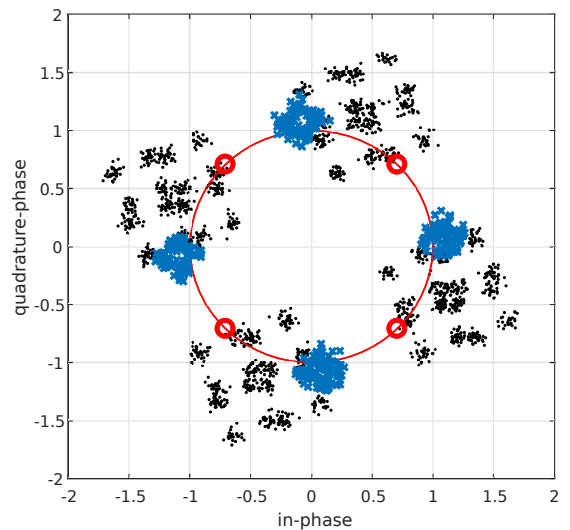


**Figure 4.5.:** RMS Expression in different IQ Imbalance, the top layer is EVM before compensation and lower layer is EVM after compensation

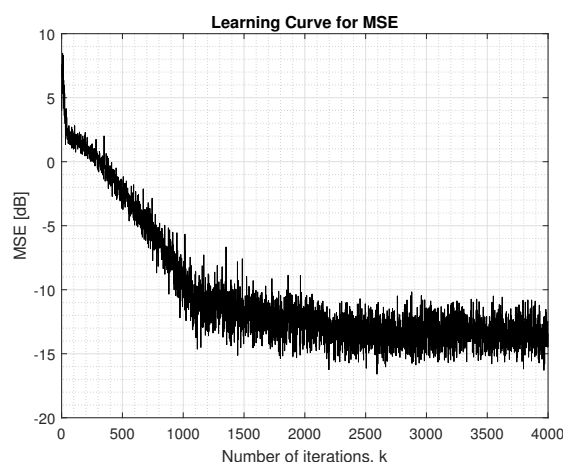
Figure 4.6a shows the constellations before and after compensator with CMA algorithm. The black points are received signal with IQ imbalance and channel distortion, while the blue points are the compensated signals. Figure 4.6b shows the convergence line through mean squared error (MSE) change by iteration. The CMA algorithm reaches convergence in about 2700 times iteration, while LMS algorithm requires only about 75 times iteration since latter algorithms as supervised method masters much more specific prior information.

Another disadvantage for the CMA algorithm is that the constant power information contains only amplitude restriction and lacks phase restriction. Therefore a phase shift is introduced as Figure 4.6(a) shows.

This phase shift can be removed by a improved algorithm called Modified CMA [30]. As shown in Figure 4.7, while the traditional CMA converges independently of carrier recovery and reaches a convergence point with a phase error, modified CMA solves this problem. Furthermore, since in modified CMA the real part and imaginary part are computed separately, the computational difficulty is actually decreased. Comparing the demand of around 2500 iterations before convergence in CMA, modified CMA converges at the fifth hundred iteration as Figure 4.7b shows. Figure 4.7 expresses the change of different weights in  $\mathbf{w}$  in each iteration. The final weight vector  $\mathbf{w} = [-0.0070 - 0.0092i, 1.2703 - 0.5877i, 0.1753 + 0.3159i, 0.1293 - 0.0460i]^T$ . Comparing to the channel distortion  $\mathbf{H} = [1.1 + j * 0.5, 0.1 - j * 0.3, -0.2 - j * 0.1]$ , the weight vector  $\mathbf{w}$  is



(a) Constellation Graph



(b) Learning / Convergence Line

**Figure 4.6.:** Equalizer with CMA Adaptive Filter for 4-QAM

closing to  $\mathbf{H}$  in someway and the rest weight ( $-0.0070 - 0.0092i$ ) convergences to zero.

#### 4.2.3. Blind Adaptive Compensator: Circularity-Based Approach

As mentioned in Chapter 3, *Lauri Anttila* proposed in 2017 a new compensation algorithm against IQ imbalance called *Circularity-based Approach* [19]. Based on widely linear processing, this blind filter presents impressive performance and compensate IQ imbalance effective.

Figure 4.8 shows the compensation result with 5dB gain imbalance and  $5^\circ$ . The convergence as shown in Figure 4.8c is  $\mathbf{w} = -0.2763 + 0.0462i$ . This makes sense because with chosen IQ imbalance of 5dB and  $5^\circ$ , the original points  $\mathbf{x}$  is actually scaled and rotated by matrix

$$M_{\text{IQImbalance}} = \begin{bmatrix} 10^{0.5 \cdot \frac{I_a}{20}} \cdot \exp(-i0.5I_p \frac{\pi}{180}) & 0 \\ 0 & 10^{-0.5 \cdot \frac{I_a}{20}} \cdot \exp(i0.5I_p \frac{\pi}{180}) \end{bmatrix} = \begin{bmatrix} 1.2995 & 0 \\ 0 & 0.6910i \end{bmatrix}, \quad (4.2)$$

where  $I_a = 5$  dB represents amplitude imbalance and  $I_p = 5^\circ$  represents phase imbalance.

The circularity-based approach adaptive filter generate a weight matrix  $M_{\text{circularity}} = \begin{bmatrix} -0.2763 & 0 \\ 0 & 0.0462i \end{bmatrix}$  to ensure that

$$\left( \begin{bmatrix} 1 & 0 \\ 0 & 0 \end{bmatrix} + M_{\text{circularity}} \right) \cdot M_{\text{IQImbalance}} = \begin{bmatrix} 0.9391 & 0 \\ 0 & 0.0321 \end{bmatrix} \approx \begin{bmatrix} 1 & 0 \\ 0 & 0 \end{bmatrix}, \quad (4.3)$$

which means the points are recovered as they were.

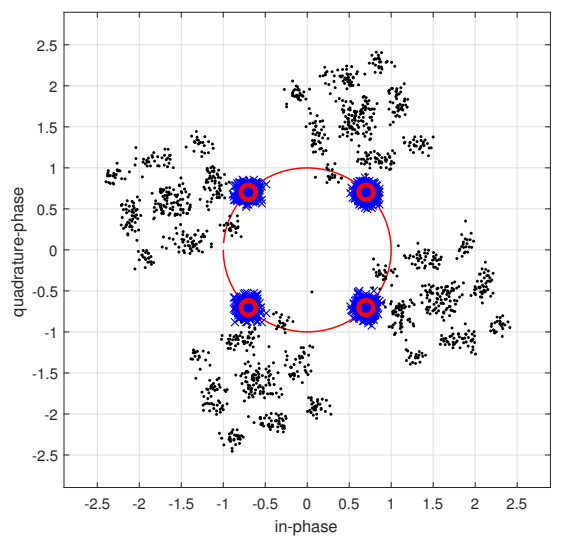
### 4.3. Impact of the Hyperparameters

Hyperparameters imply the setting parameters before adaptive filters start. Basic hyperparameters in filters contain normally equalizer length  $N$ , iteration step length  $\mu$  and iteration times. By iteration times we choose a large number to ensure reaching the convergence point. However, chooses of equalizer length and iteration step length are following experience and experiments.

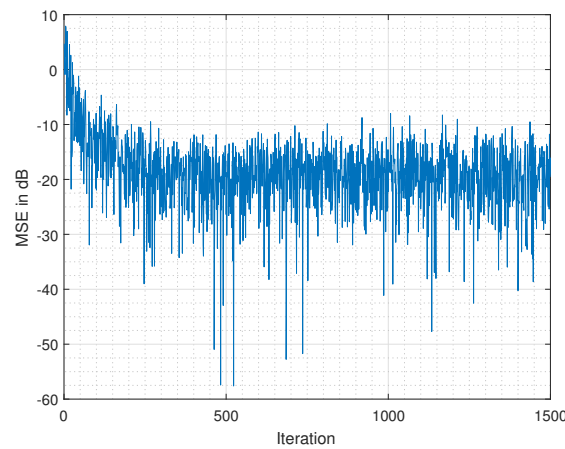
The influence of filter length  $N$  is shown in Figure 4.9. MSE moves are processed by moving average in the consideration of clearness.

On the one hand, dealing with channel distortion  $\mathbf{H} = [1.1 + j * 0.5, \quad 0.1 - j * 0.3, \quad -0.2 - j * 0.1]$ , since channel contains three taps, the LMS filter with  $N > 3$  performs obviously better than  $N \leq 3$ . MSE is reduced to about  $-28$  dB by 5 ordered LMS filter, while by lower length MSE reaches only to  $-5$  dB ( $N = 1$ ) and to  $-16$  dB.

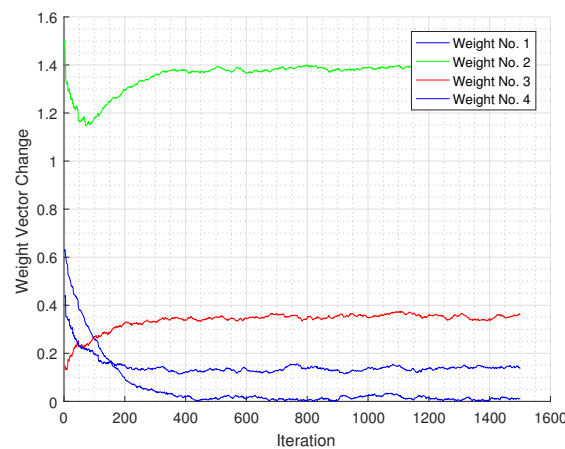
On the other hand, Figure 4.9 also shows filter with lower length has higher convergence speed. LMS filter with  $N = 5$  converges at second thousand times iteration, while the one



(a) Constellation Graph

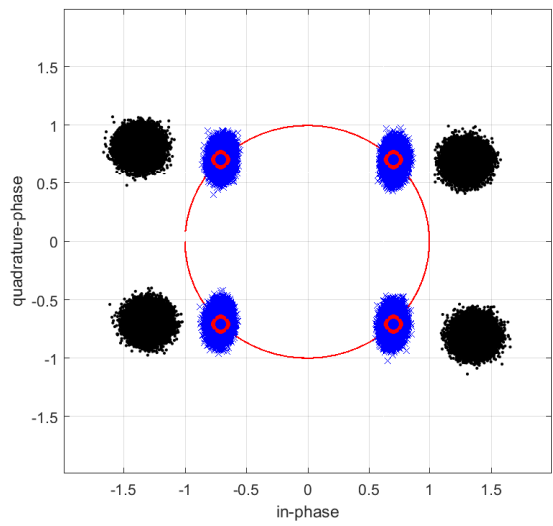


(b) Learning / Convergence Line

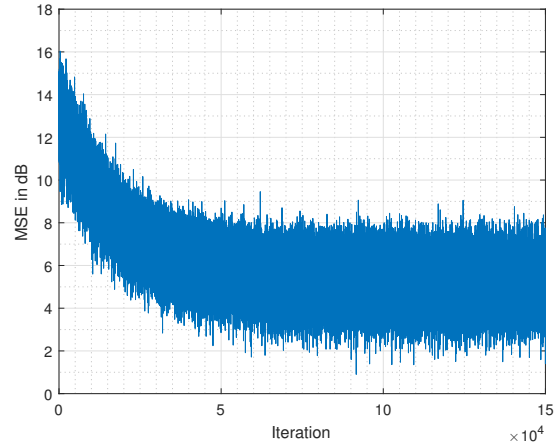


(c) Weight Vector changes during iterations

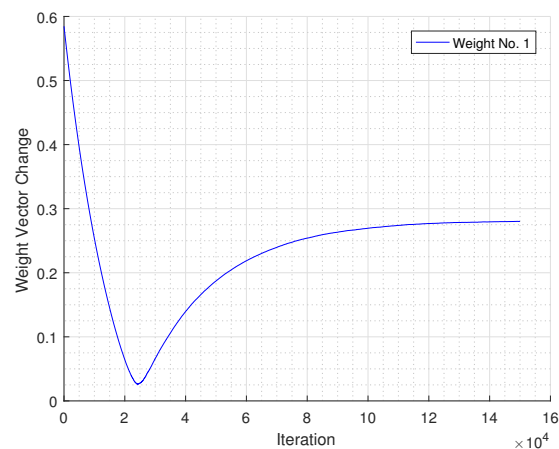
**Figure 4.7.:** Equalizer with Modified CMA Adaptive Filter for 4-QAM



(a) Constellation Graph



(b) Learning / Convergence Line



(c) Convergence Process of Weight

**Figure 4.8.: Equalizer with Circularity-Based Approach Filter for 4-QAM**

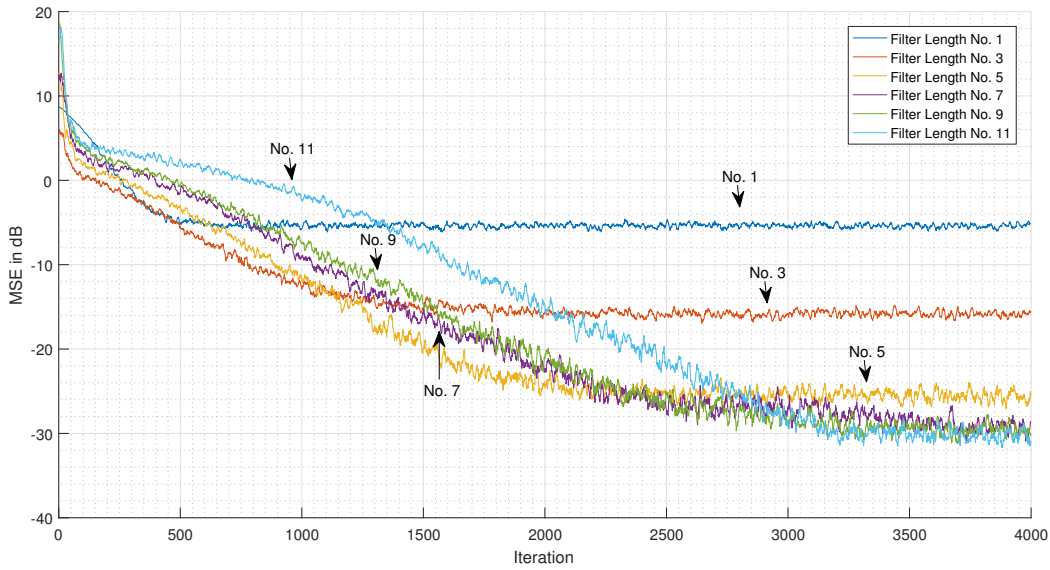


**Figure 4.9.**: MSE of CMA filter in different filter length  $N$

with  $N = 11$  reaches convergence point at third thousand times iteration, although its MSE is controlled 4 dB better (from  $-26$  dB to  $-30$  dB). Therefore a trade-off of filter length  $N$  should be noticed.

Another hyperparameter iteration step length  $\mu$  controls the step value of each movement. Large step length will increase the convergence speed. As Figure 4.10a shows, by step length  $\mu = 0.001$  it takes 800 iterations for the convergence, while under 100 iterations are demanded by step length  $\mu = 0.015$ .

However, some disadvantages are introduced by large step length at the same time. Large step length causes not only a rough convergence with an always changing weight vector  $\mathbf{w}$ , but the filter becomes also unstable and easy divergences. When the filter diverges, weight vector  $\mathbf{w}$  becomes infinitely large and totally unusable. Figure 4.10b shows this situation. Although the weight enters the desired area, comparing to  $\mu = 0.001$ , it walks around the optimal point in a large circus. Optimal weight vector can not be precise estimated because of large step chose.

To the contrary, Figure 4.10c shows what happened if step length  $\mu$  is too small. After 1500 iterations the weight vector  $\mathbf{w}$  still doesn't reach the convergence point. This will waste compute resource and increase computational cost.

#### 4.4. Computational Load and Impact of time-varying channels

The study of tracking ability is also important for proposed equalizers. Compare to fixed filters, adaptive filters are able to adjust weight parameters and adapt time-varying channel, if the

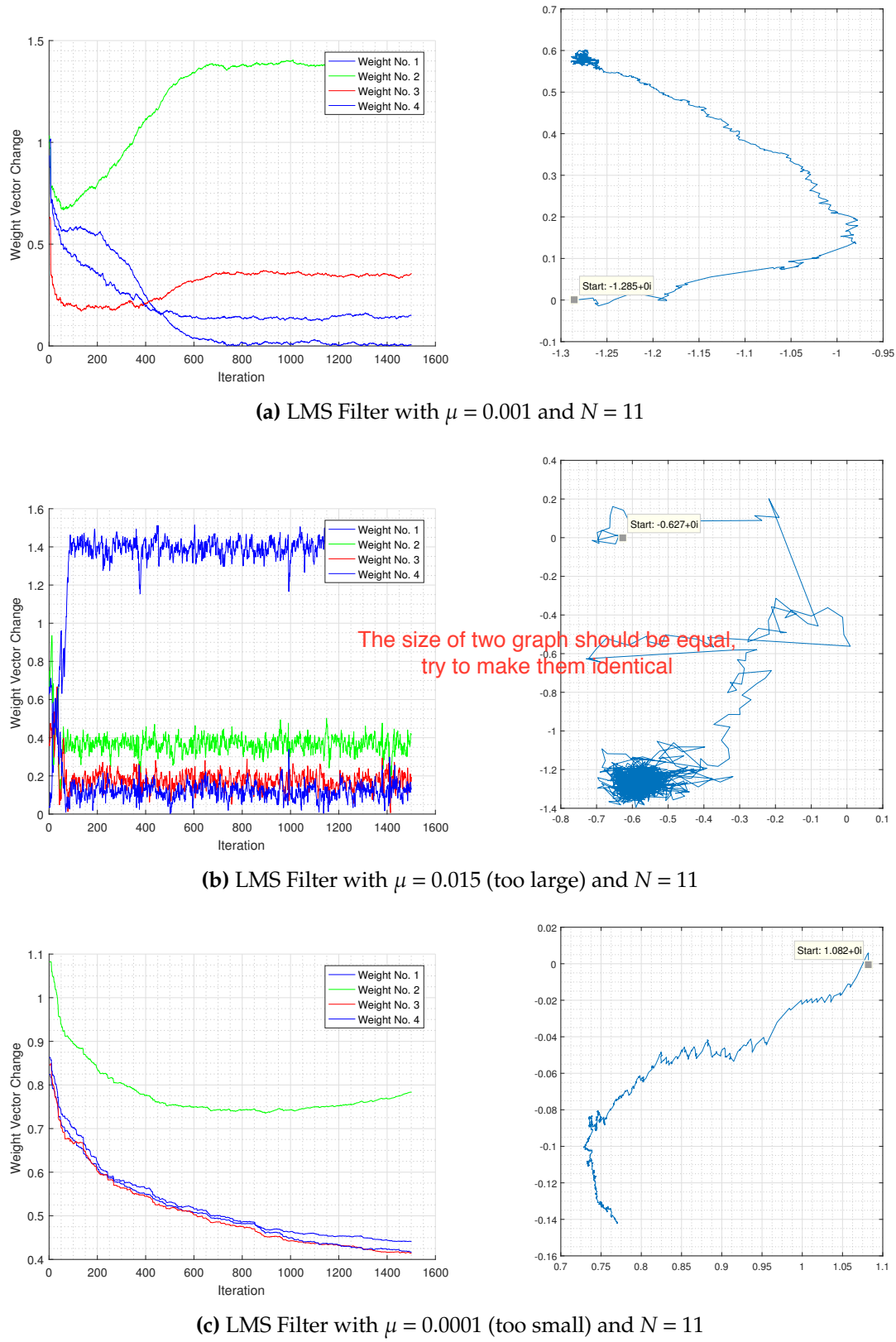


Figure 4.10.: Convergence Results for Different Step Size

impairments change relatively gently.

For the sake of simplicity, only infinite polarization rotation by the Jones matrix is considered. The channel impulse response at time  $t_0$  can be written as

$$\mathbf{C}_{t_0}(t) = \begin{bmatrix} \cos(\Omega t_0) & \sin(\Omega t_0) \\ -\sin(\Omega t_0) & \cos(\Omega t_0) \end{bmatrix} \delta(t), \quad (4.4)$$

where  $\Omega$  is the rotation speed in  $\text{rad s}^{-1}$ .

In consideration of limited computational power in reality, the complexity of various algorithms is also a critical part for implementation of real time communication. The compute time cost is shown in Table 4.2. All adaptive filters are trained (for supervised filters) with 300 symbols and tested with  $10^5$  symbols. The convergence process takes time, especially for circularity-based approach because of its huge iteration demand. After convergence things become easier. With consideration of big test set, a processing time of about 1 ms is not expensive. Of course, all computer works are done in a general PC. As to practice, such a computational ability might be out of possession. Some more practical measurement should be proposed.

	LMS	RMS	CMA	Modified CMA	Circularity-based Approach
Iteration demand	100	70	3000	500	$10^5$
Each iteration ( $\mu\text{s}$ )	8	9	8	8	8
Initial Time (ms)	0.8	0.63	24	4	800
Use Time for $10^5$ symbols (ms)	1.013	1.012	0.997	1.005	0.472
Computational Complexity	$2N+1$	$4N^2$	$2(4N+1)$		

**Table 4.2.:** Time Cost for Different Adaptive Filters (with optimal hyperparameters), 4-QAM

## 4.5. KNN and SVM Detectors

As mentioned in Chapter 3, SVM and KNN are data-aided detectors. The performance of KNN is shown in Figure 4.11. In the small phase noise level range  $-35$  to  $-45 \text{ dBHz}^{-1}$ , KNN can reduces about 50 % symbol errors.

The modulation is 16 QAM and received signal as Figure 4.12 shows is distorted by phase noise with frequency offset  $f_{\text{offset}} = 10 \text{ Hz}$  and phase noise level  $L = -40 \text{ dBc/Hz}$ . The number of training symbols is kept as 100. Figure 4.13 shows classified areas with various labels according to training symbols. The different colored blocks represent different decisions. It takes 0.787 s to train SVM. Once training finished, SVM can detect the symbol immediately.

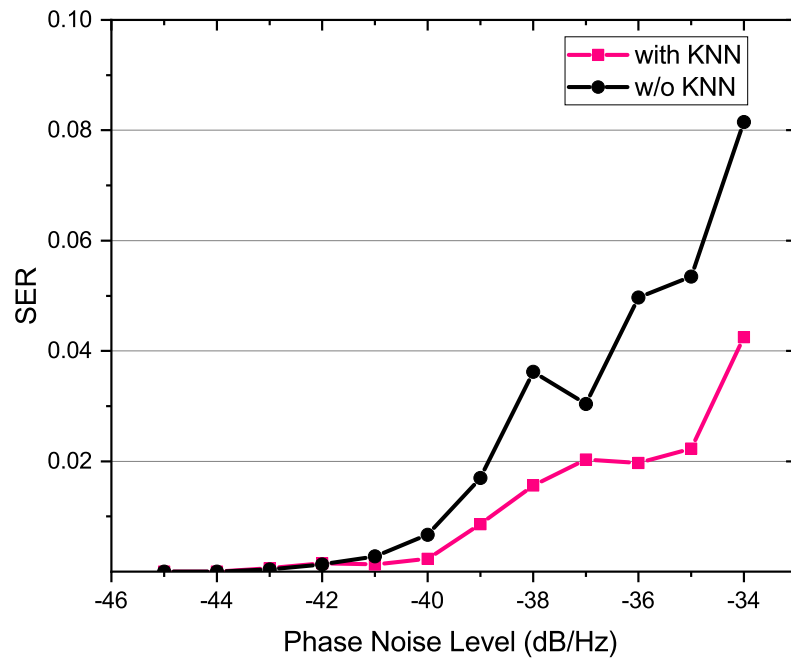


Figure 4.11.: SER with and w/o KNN Detector

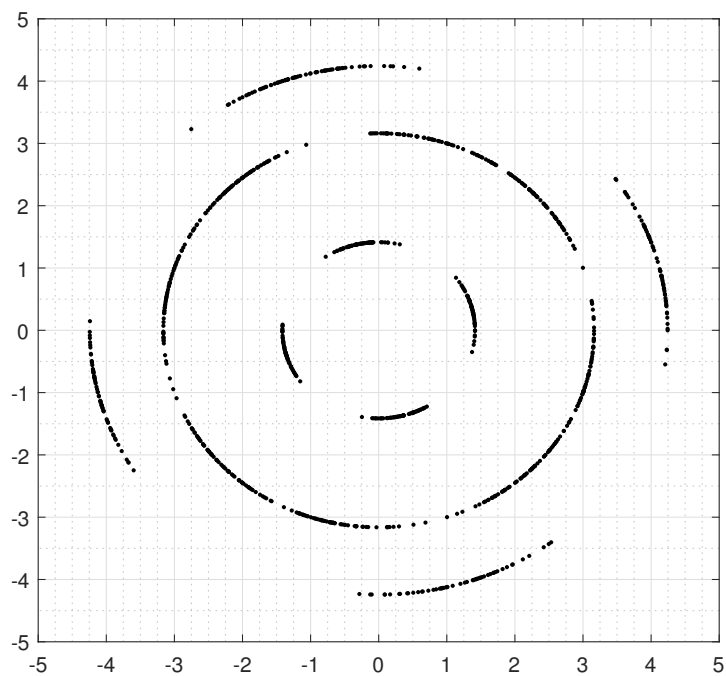


Figure 4.12.: RX Constellation Points with Phase Noise Impairment



**Figure 4.13.:** Detection of SVM against Phase Noise Impairment

Here are only graph, try to mix the page with graph and text, only graph is not so much good

## 5. Conclusion and Perspectives

Newer and more demanding wireless applications are pushing the telecommunication technology forward. Increasing speed need ask for high signal quality, which though is hard to satisfy because of the crowded radio spectrum and limited spectrum resource. Besides hardware design and coding technology (check bit or self-correcting code), some post-end technology makes also the contribution.

The work carried out in the thesis deals with both deterministic impairments (channel distortion, IQ imbalance) and stochastic impairment (phase noise). Channel distortion merge old symbols and new symbol by deterministic weights. In addition, fixed or slow changing scaling and phase shifting are also convoluted in the transmitted signal through IQ imbalance. Deterministic impairments are relatively easy to equalize since once we get weight vector, compensation can be done with a satisfied result. By contrast, stochastic impairment phase noise is more difficult to eliminate. Even if the parameters are known, we can still not equalize each point precisely.

Furthermore, we introduced several algorithms and methods for improving the whole system. Higher and more powerful chips are also making potential algorithms more possible than any other moment in history. For deterministic impairments, we use basically gradient-descent algorithm through constant step-size version to approach weight vector. Different cost functions bring a huge difference in convergence speed, final MSE, and computational complexity. We discuss in detail the chose and its effect of step size  $\mu$ , filter length  $L$  and iteration number  $N$ .

For stochastic impairment phase noise, we try new methods SVM and KNN. In this article we mainly realize SVM as recognizer [24]. After training by initial symbols, SVM separate the constellation area properly. Newly received symbols are demodulated to different labels according to this separation.



## Bibliography

- [1] *Attenuation by atmospheric gases, Recommendation ITU-R P.676-11, P Series, Radiowave propagation.* International Telecommunication Union, 2016.
- [2] "Cisco visual networking index: Global mobile data traffic forecast update, 2016–2021 white paper."
- [3] B. Feldman, *The Nobel Prize: a history of genius, controversy, and prestige.* Arcade Publishing, 2001.
- [4] "IMT vision – framework and overall objectives of the future development of IMT for 2020 and beyond," p. 21.
- [5] "E-band frequency licensing - e-band communications, LLC."
- [6] F. C. Commission, "Allocations and service rules for the 71-76 ghz, 81-86 ghz and 92-95 ghz bands order."
- [7] "United states frequency allocation chart | national telecommunications and information administration."
- [8] A. Grami, *Introduction to Digital Communications.* Academic Press. Google-Books-ID: 6nww-BAAAQBAJ.
- [9] T. H. Lee, *The Design of CMOS Radio-Frequency Integrated Circuits.* Cambridge University Press, 2 ed., 2003.
- [10] A. A. Abidi, "Direct-conversion radio transceivers for digital communications," *IEEE Journal of Solid-State Circuits*, vol. 30, pp. 1399–1410, Dec 1995.
- [11] S. Sharma, J. Nagar, and P. Singh, "Modeling and performance analysis of wireless channel," in *2016 3rd International Conference on Computing for Sustainable Global Development (INDIACom)*, pp. 3052–3057.
- [12] "The RF and microwave handbook."
- [13] Q. Gu, *RF System Design of Transceivers for Wireless Communications.* Springer US.
- [14] K. M. Gharaibeh, *Nonlinear Distortion in Wireless Systems: Modeling and Simulation with MATLAB.* John Wiley & Sons. Google-Books-ID: EMI2xW9gqLQC.
- [15] K. McClaning and T. Vito, *Radio Receiver Design.* Noble Publishing Corporation. Google-Books-ID: 6hEfAQAAIAAJ.
- [16] B. Razavi, *RF Microelectronics.* Prentice Hall. Google-Books-ID: \_TccKQEACAAJ.
- [17] M. McKinley, C. A. Remley, M. Myslinski, and J. S. Kenney, "EVM calculation for broadband modulated signals,"

- [18] D. B. Leeson, "A simple model of feedback oscillator noise spectrum," vol. 54, no. 2, pp. 329–330.
- [19] L. Anttila, M. Valkama, and M. Renfors, "Blind compensation of frequency-selective i/q imbalances in quadrature radio receivers: Circularity -based approach," in *2007 IEEE International Conference on Acoustics, Speech and Signal Processing - ICASSP '07*, vol. 3, pp. III–245–III–248.
- [20] D. GODARD, "Self-recovering equalization and carrier tracking in two-dimensional data communication systems," vol. 28, pp. 1867–1875.
- [21] R. Johnson, P. Schniter, T. J. Endres, J. D. Behm, D. R. Brown, and R. A. Casas, "Blind equalization using the constant modulus criterion: a review," vol. 86, no. 10, pp. 1927–1950.
- [22] P. S. R. Diniz, *Adaptive Filtering: Algorithms and Practical Implementation*. Springer US, 4 ed.
- [23] D. Wang, M. Zhang, M. Fu, Z. Cai, Z. Li, H. Han, Y. Cui, and B. Luo, "Nonlinearity mitigation using a machine learning detector based on  $k$ -nearest neighbors," vol. 28, no. 19, pp. 2102–2105.
- [24] D. Wang, M. Zhang, Z. Cai, Y. Cui, Z. Li, H. Han, M. Fu, and B. Luo, "Combatting nonlinear phase noise in coherent optical systems with an optimized decision processor based on machine learning," vol. 369, pp. 199–208.
- [25] S. Tong and D. Koller, "Support vector machine active learning with applications to text classification," vol. 2, pp. 45–66.
- [26] R. O. Duda, P. E. Hart, and D. G. Stork, *Pattern Classification*. Wiley-Interscience, 2. ed.
- [27] V. Vapnik, *The Nature of Statistical Learning Theory*. Information Science and Statistics, Springer-Verlag, 2 ed.
- [28] "Advanced design system (ADS) | keysight (formerly agilent's electronic measurement)."
- [29] S. J. Savory, "Digital coherent optical receivers: Algorithms and subsystems," vol. 16, no. 5, pp. 1164–1179.
- [30] K. N. Oh and Y. O. Chin, "Modified constant modulus algorithm: blind equalization and carrier phase recovery algorithm," in *ICC '95 Seattle, 'Gateway to Globalization', 1995 IEEE International Conference on Communications, 1995*, vol. 1, pp. 498–502 vol.1.

# **Appendices**



## A. Acknowledgments

I would like to gratefully acknowledge the people who supported me and who have contributed directly or indirectly, to my work and my personal development.

Firstly, I would like to thank Prof. Dr.-Ing. Ingmar Kallfass, for giving me the opportunity to write my Research Thesis in his research group and take advantage of knowledge and experience. I am also grateful to my thesis adviser M.Sc. Seyyid Muhammed Dilek for introducing me into this attractive and fantastic topic, often support and encourages during long path to knowledge. Without his patient instruction, insightful criticism and expert guidance, the completion of this thesis would not have been possible. Furthermore, his kindness and friendship make everywhere full of warm and motivation in the students room.

From Institute of Robust Power Semiconductor Systems (*Institut für Robuste Leistungshalbleitersysteme*, ILH) also, I would like to thank Mr. Rui Li, Mr. Xiangge Deng, Mr. Tailang Xie, Mr. Tianyu Cheng, Ms. Man Mei and Ms. Bingnan Liu. They either solved strange problems of various softwares for me, or raised conceptual questions in a way I will never consider, which always makes me to think more thoroughly and comprehensive.

The passion for microwave engineering would have never been so deep without unforgettable experience in ILH. I am really thankful to the help and motivation from ILH.



## B. Script Flow Chat

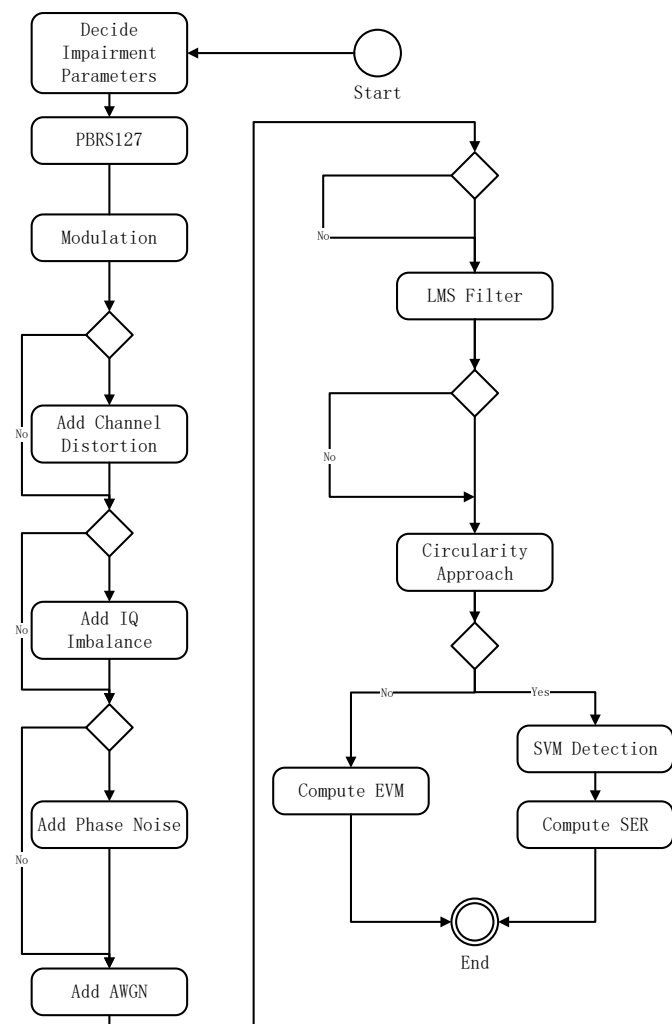


**Figure .1.: Script Flow Chat**



## C. Simulation Results

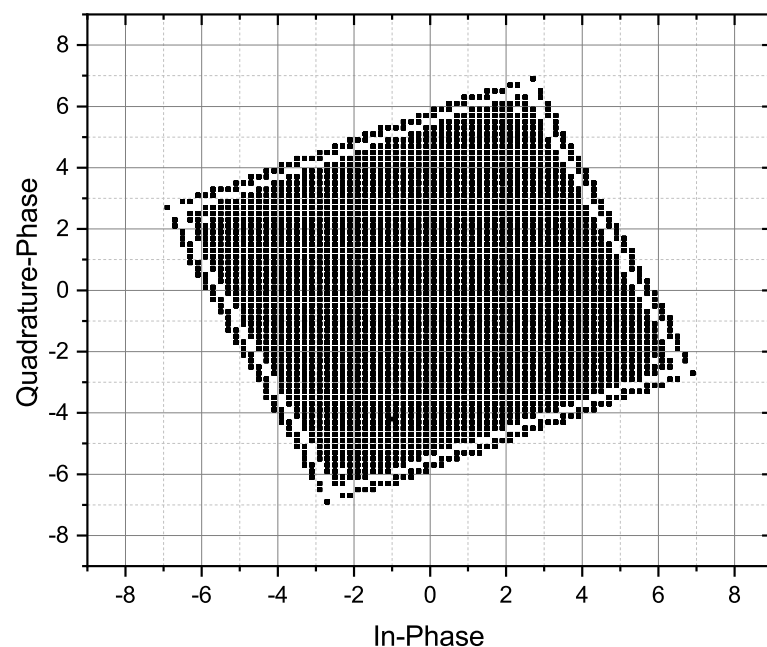


**Figure .1.:** Signal with Channel Distortion

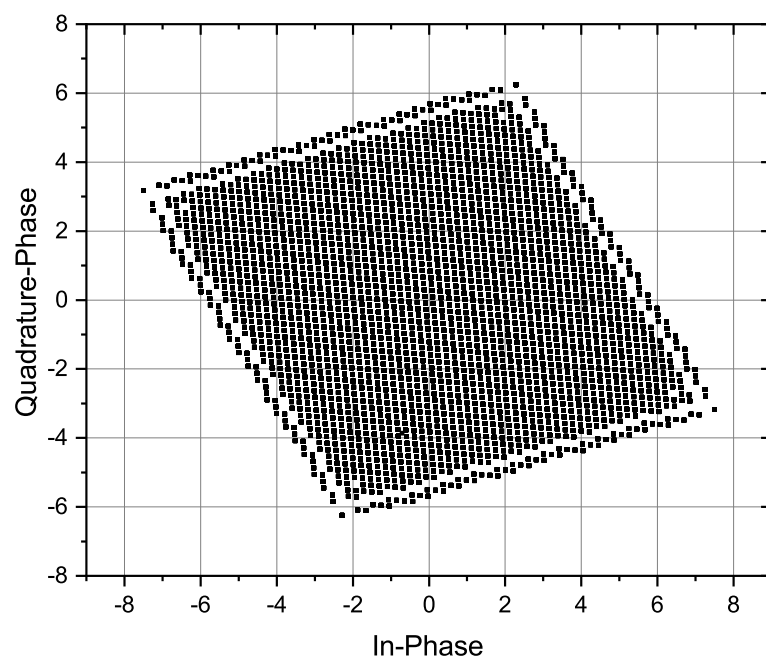


**Figure .2.:** Signal with IQ Imbalance

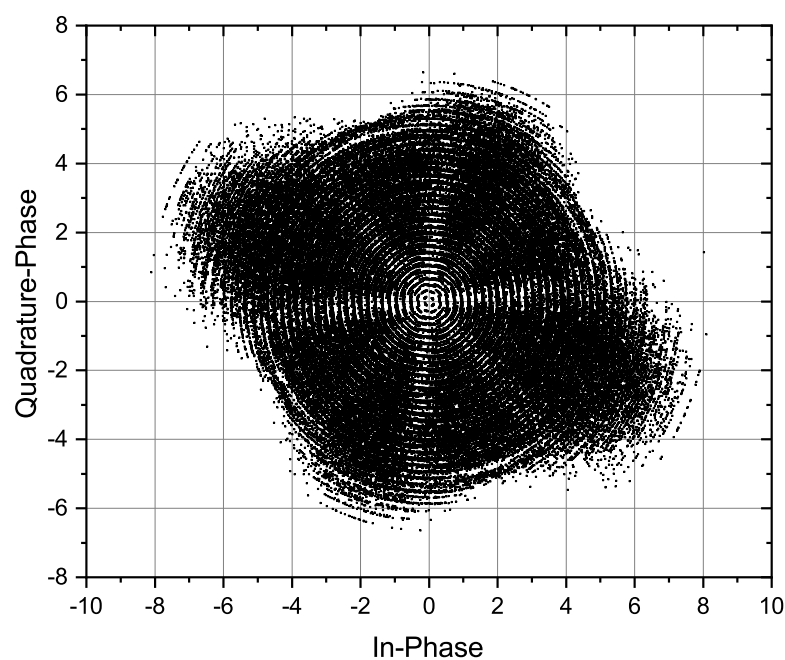


**Figure .3.:** Signal with Phase Noise

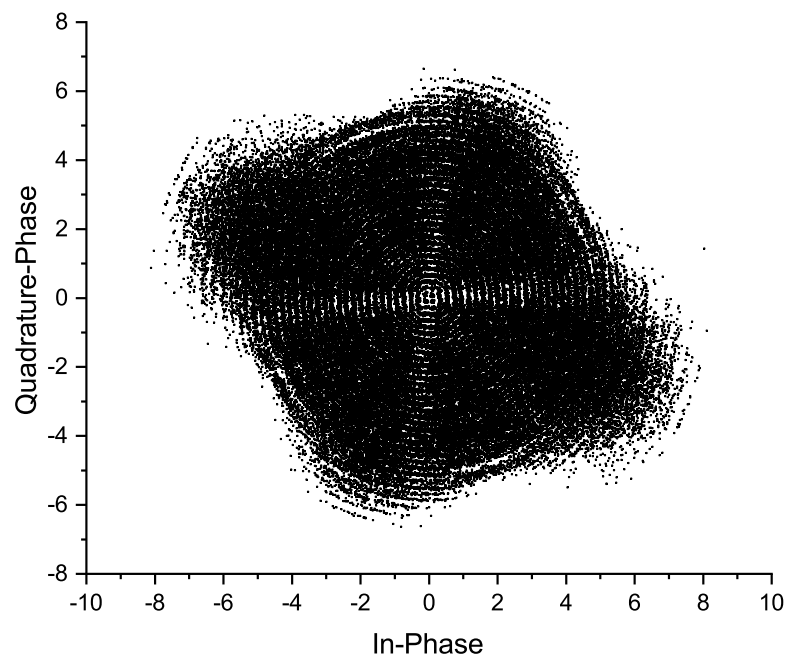


**Figure .4.:** Signal with AWGN

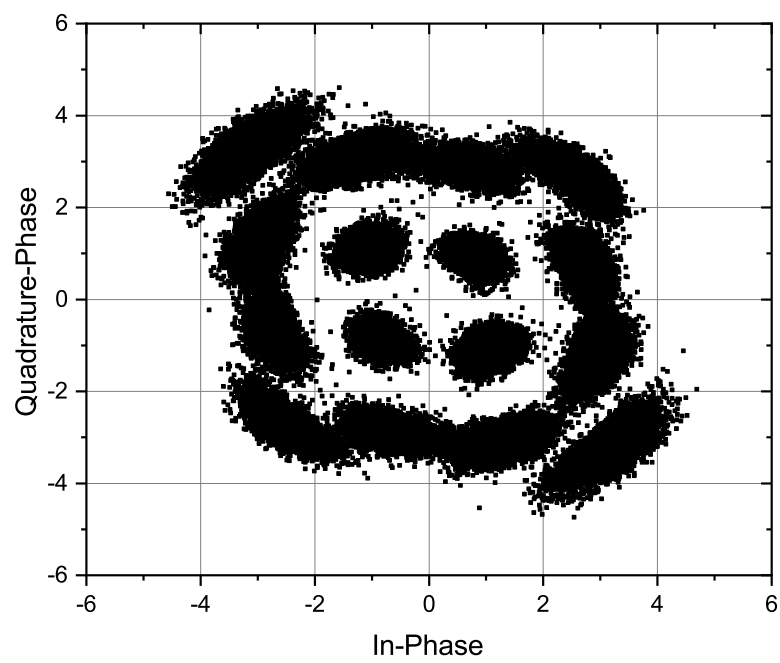


**Figure .5.:** Signal Compensated by LMS Filter

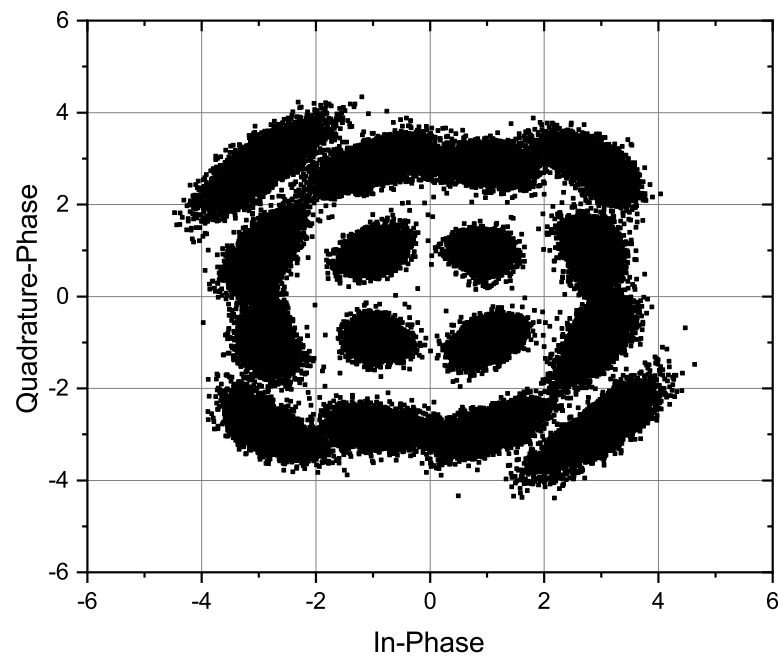


**Figure .6.:** Signal Compensated by Circularity Approach

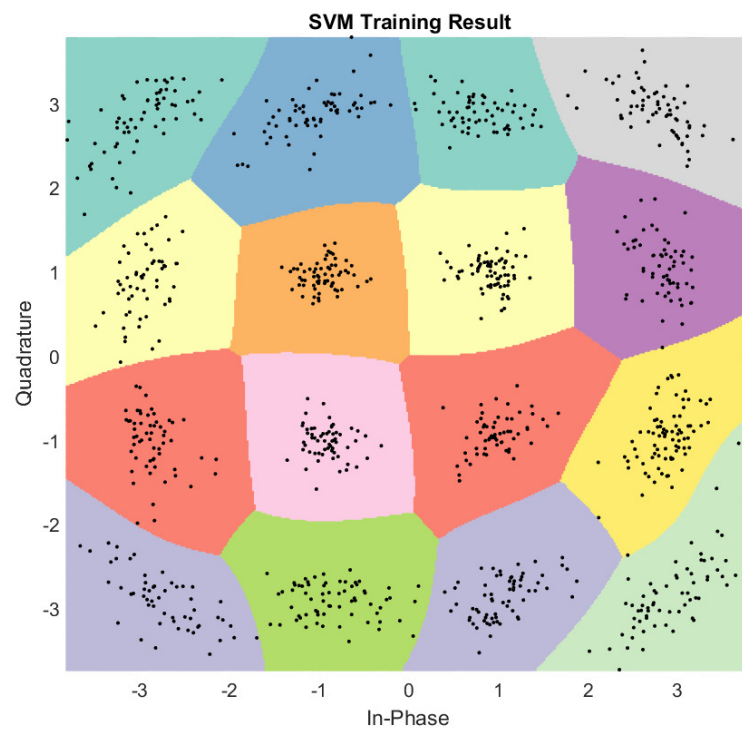
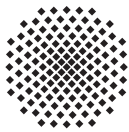


**Figure .7.:** SVM Recognize



**Yang Liu**

**Student Research Project: Mmwave Transceiver System Performance Analysis using Post-Processing Analysis**

**Period: Still didn't find a way to delete it – 31.07.2018**

**Supervisor: Prof. Dr.-Ing. Ingmar Kallfass , M. Sc. Seyyid Muhammed Dilek**

**Executive Abstract:** Performance enhancement of a millimeter-wave transceiver system is a challenging problem in modern radio ranging, detection, and communication applications which in fact make this problem motivational to work on. Digital post-processing techniques which use adaptive equalization filters are an important way to improve performance for broadband millimeter-wave wireless transceiver system. Digital post-processing methods can dramatically improve the performance of the received digital baseband signal and, furthermore, it can mitigate the analog front-ends and channel impairments influence. Analog front-ends and channel non-idealities for transceiver systems concern the performance degradation of the signal quality. There are various ways for the mitigation techniques which is explained in this research thesis.

The growth of Internet traffic and network connections are driving researchers towards millimeter-wave between 30 GHz and 300 GHz. Among this RF range, E-band (71-76 GHz and 81-86 GHz) receives particular attention and provides new potentials and challenges for providing affordable and reliable point-point communications with data rates up to  $10 \text{ Gbits}^{-1}$ . However, higher frequencies of mmW raise strong requirements on low transmission distortion and high impairment mitigation ability at pose-end. This thesis first reviews the available bandwidth and regulation in the E-band. Subsequently, different analog front-ends and channel impairments are studied along the causes and classifications.

Based on properties and classifications, applicable post-processing methods are realized and simulated to evaluate its performance. For deterministic impairments, linear adaptive filters, including LMS, RMS, CMA etc. performance a satisfied improvement after convergence. For stochastic impairments, basic machine learning method such as KNN and SVM are tested as a primary trial. Several distortions are equalized effectively and EVM is reduced from 34 % to 4 %. In the consideration of practice, optimized parameters and recommendations are given. Different adaptive algorithms are also compared in terms of computational load. Finally, it is argued that the related post-processing methods can be used to enhance the performance of broad-band mmW transceiver system, although the algorithms in the application should be optimized to reduce the computational complexity.